Research article

An application of aromatic compounds as alternative tracers of tsunami backwash deposits

Siwatt Pongpiachan [a,b,c,*], Vanisa Surapipith [c], Muhammad Zaffar Hashmi [d], Suparerk Aukkaravittayapun [c], Saran Poshyachinda [c]

[a] NIDA Center for Research & Development of Disaster Prevention & Management, School of Social and Environmental Development, National Institute of Development Administration (NIDA), 118 Moo-3, Sereethai Road, Klong-Chan, Bangkapi, Bangkok 10240 Thailand
[b] SKLLQG, Institute of Earth Environment, Chinese Academy of Sciences (IEECAS), Xi'an, 710075, China
[c] National Astronomical Research Institute of Thailand (Public Organization) (NARIT), 260 Moo 4, T. Donkaew, A. Maerim, Chiangmai, 50180, Thailand
[d] Department of Chemistry, COMSATS University Islamabad, 44000, Pakistan

A B S T R A C T

This manuscript provides some comprehensive technical insights regarding the application of polycyclic aromatic hydrocarbons (PAHs) characterized by using Gas-Chromatography Mass Spectrometry. Although numerous chemical species such as water soluble ionic species (e.g. Na^+, K^+, Cl^-, Ca^{2+}, Mg^{2+}) and acid leachable heavy metal fractions (e.g. Fe, Cd, Al, Mo, Sb, As, Cu, Zn, Pb, and Mn) can be used to characterize tsunami deposits, the knowledge of PAH congeners as alternative chemical species for identifying tsunami backwash deposits is strictly limited. This manuscript is exclusive because it aims to find some alternative chemical proxies in order to distinguish tsunami backwash deposits from typical marine sediments. A wide range of diagnostic binary ratios of PAH congeners have been selected in order to characterize Typical Marine Sediments (TMS), Tsunami backwash deposits (TBD), Onshore Tsunami Deposits (OTD) and Coastal Zone Soils (CZS). The state of the art and future perspectives coupled with both advantages and disadvantages of above mentioned chemical tracers will be critically reviewed and further discussed.

1. Introduction

1.1. Research background

During the past few decades, geoscientists have relied on an array of physical evidences, such as uncommonly coarse grain size in comparison to neighboring sediments, the complicated sources of deposits, unique vertical and horizontal fluctuations in particle size composition, are all regarded as typical diagnostic aspects of tsunami backwash deposits (Bellanova et al., 2020b; Cantalamessa and Di Celma, 2005; Goto et al., 2019; Ishizawa et al., 2020; Shi et al., 1995). Some distinctive features of tsunami deposits can be considered as several consequences of the processes of tsunami generation, propagation, and the sedimentary responses (Dawson and Stewart, 2007). In spite of numerous efforts on characterizing sedimentary features of tsunami backwash deposits offshore and historic tsunami onshore by using geophysical records, there were only few studies using geochemical tracers such as water soluble ionic species, heavy metals and polycyclic aromatic hydrocarbons

(PAHs) in order to investigate the tsunami evidences (Goto et al., 2011; Irizuki et al., 2019; Pongpiachan et al., 2013a,b,c,d,e; Pongpiachan, 2014; Prasath and Khan, 2008; Szczuciński et al., 2005, 2007; Tipmanee et al., 2012; Watanabe et al., 2020). It was found that the 2011 Tohoku-oki tsunami deposits contained comparatively high contents of water-soluble chloride which can be applied as geochemical tracers for investigating historic tsunami (Goto et al., 2011). According to the applications of geochemical tracers, historic tsunami (e.g. 869 AD Jōgan earthquake and tsunami) in Sendai plain, Japan have seemingly been miscalculated. If the 2011 and 869 AD tsunami episodes are undeniably equivalent, the risk from tsunami in Japan is considerably larger than formerly acknowledged (Goto et al., 2011).

Similar patterns were previously observed in marine deposits in tsunami-inundated area triggered by the 26 December 2004 Indian Ocean tsunami wave (Szczuciński et al., 2005). Some prominent features such as the enrichment of ionic species (e.g. Na^+, K^+, Ca^{+2}, Mg^{+2}, Cl^- and SO_4^{-2}) in water-soluble fraction, and heavy metals (e.g. Cd, Cu, Zn, and Pb) in the bioavailable fraction were detected in all surface and

---

* Corresponding author.
  E-mail address: pongpiajun@gmail.com (S. Pongpiachan).

Table 1. Chemical structures of PAHs.

Congener	Abbreviation	M.W. [g]	Chemical Structure
Acenaphthylene	Ac	152	
Acenaphthene	Ace	154	
Fluorene	Fl	166	
Phenanthrene	Phe	178	
Anthracene	An	178	
3-Methyl Phenanthrene	3-MePhe	192	
9-Methyl Phenanthrene	9-MePhe	192	
1-Methyl Phenanthrene	1-MePhe	192	
2-Methyl Phenanthrene	2-MePhe	192	
1-methyl-7-isopropyl phenanthrene (Retene)	Ret	234	
Fluoranthene	Fluo	202	
Pyrene	Py	202	

Table 1 (*continued*)

Congener	Abbreviation	M.W. [g]	Chemical Structure
Benz[*a*]anthracene	B[*a*]A	228	
Chrysene	Chry	228	
Triphenylene	Tri	228	
Benzo[*b*]fluoranthene	B[*b*]F	252	
Benzo[*j*]fluoranthene	B[*j*]F	252	
Benzo[*k*]fluoranthene	B[*k*]F	252	
Benzo[*e*]pyrene	B[*e*]P	252	
Benzo[*a*]pyrene	B[*a*]P	252	
Perylene	Per	252	
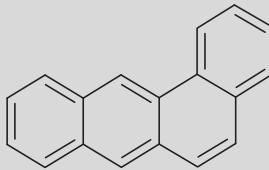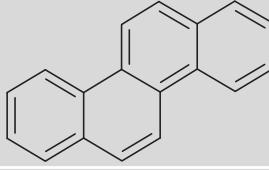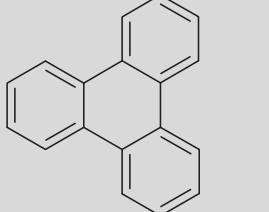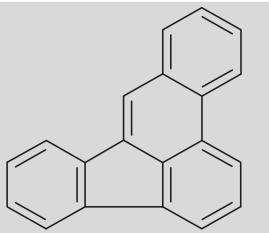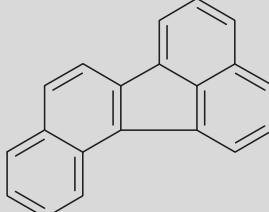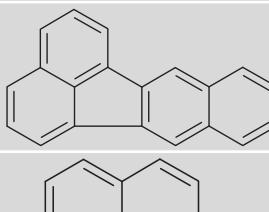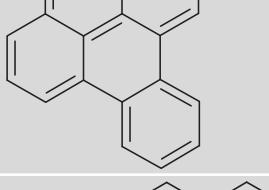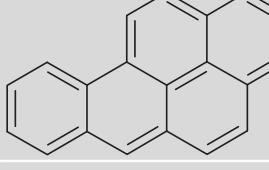
Table 1 (*continued*)
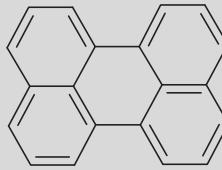
Congener	Abbreviation	M.W. [g]	Chemical Structure
Indeno[*1,2,3-cd*]pyrene	Ind	276	
Benzo[*g,h,i*]perylene	B[*g,h,i*]P	276	
Anthanthrene	Ant	276	
Dibenzo[*a,h*]anthracene	D[*a,h*]A	278	
Coronene	Cor	300	
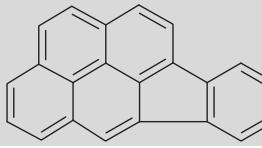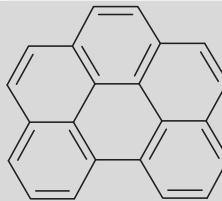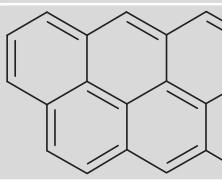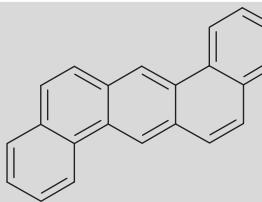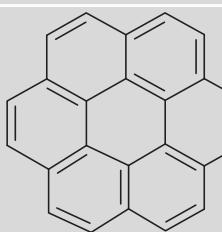
ground waters in tsunami-inundated zone at the Southern part of Thailand (Szczuciński et al., 2005). These scientific evidences indicated that unexpectedly large tsunami inundation can cause adverse health effects since there is a danger of transfer of heavy metals into ground waters and potential bioaccumulation and/or biomagnification along the aquatic food chain. However, it is also crucial to underline that these results are site-specific and could be influenced by many anthropogenic factors. For instance, there was exploration and mining activities in the vicinity of Bang More village and Nam Khem village, which were carefully selected as sampling sites (Szczuciński et al., 2005). A more comprehensive review associated with the applications of geochemistry as markers of marine inundation for investigations of the limit of tsunami inundation has been reported by Chagué-Goff et al., 2017. Several geochemical proxies such as water-leachable ions coupled with carbonates (Minoura et al., 1987; Minoura and Nakata, 1994; Minoura and Nakaya, 1991), DNA (Somboonna et al., 2014; Szczuciński et al., 2016), major and trace elements (Jayawardana et al., 2012), total organic carbon coupled with stable isotope (i.e. TOC, TN, C/N, $\delta^{13}C$, $\delta^{15}N$) (Dahanayake et al., 2012), elemental counts (Sakuna et al., 2012), organic functional groups as characterized by Fourier-transform infrared

spectroscopy (FTIR) (Pongpiachan et al., 2013b), and μ-SXRF spectra of elements (Pongpiachan et al., 2013c) have been introduced as promising geochemical markers for evaluating the impacts of tsunami inundation (Chagué-Goff et al., 2017). The most recent publication underlined the importance of geochemical proxy (e.g. Ca/Ti and Sr/Ba) coupled with diatom assemblages with grain sizes characteristics to describe the tsunami deposits and its maximum inundation limit occurred on 27th February 2010, at Las Cañas, Maule Region, Chile (Chagué-Goff et al., 2015). Further attempts have also been focused on identifying the evidence of small historical tsunamis in Lyttelton Harbour, New Zealand by applying a multi-proxy approach comprising sedimentological, geochemical and diatom analyses complemented by dating from ^{137}Cs activity profiles and historical data (Judd et al., 2017). Numerous types of multiproxy such as anhysteretic remanent magnetization (ARM), anisotropy of magnetic susceptibility (AMS), and X-ray fluorescence (XRF) were used to investigate the signature of the 1755 tsunami deposit at Boca do Rio, Algarve, Portugal (Moreira et al., 2017; Vigliotti et al., 2019).

Recent studies have highlighted the importance of anthropogenic organic substances (e.g. PAHs, halogenated aromatics, soil derived

Table 2. Sediment sampling positions and water depths.

Sample No.	Date	Latitude	Longitude	Water depth (m)
011207–01	01.12.07	08° 50.964′	97° 58.394′	60.15
011207–02	01.12.07	08° 50.940′	98° 01.754′	53.20
011207–03	01.12.07	08° 50.905′	98° 02.101′	52.40
011207–04	01.12.07	08° 49.975′	98° 04.002′	49.20
011207–05	01.12.07	08° 50.945′	98° 03.650′	49.20
011207–06	01.12.07	08° 50.861′	98° 05.808′	39.70
011207–07	01.12.07	08° 51.082′	98° 06.085′	38.85
011207–08	01.12.07	08° 51.050′	98° 07.638′	31.30
011207–09	01.12.07	08° 50.977′	98° 09.736′	22.50
011207–10	01.12.07	08° 50.953′	98° 11.688′	18.00
021207–11	02.12.07	08° 46.901′	98° 11.512′	20.10
021207–12	02.12.07	08° 47.459′	98° 11.528′	20.10
021207–14	02.12.07	08° 50.189′	98° 11.433′	18.70
021207–15	02.12.07	08° 48.964′	98° 06.893′	35.90
021207–16	02.12.07	08° 48.147′	98° 04.652′	44.70
021207–17	02.12.07	08° 47.607′	98° 03.969′	44.40
021207–18	02.12.07	08° 49.088′	98° 02.357′	52.10
021207–19	02.12.07	08° 49.310′	98° 00.351′	56.90
021207–20	02.12.07	08° 49.296′	97° 59.819′	57.80
031207–21	03.12.07	08° 45.989′	97° 58.549′	63.40
031207–22	03.12.07	08° 46.867′	97° 59.167′	61.80
031207–23	03.12.07	08° 44.940′	98° 01.167′	56.50
031207–24	03.12.07	08° 44.929′	98° 02.555′	52.30
031207–25	03.12.07	08° 45.978′	98° 04.280′	44.10
031207–26	03.12.07	08° 47.278′	98° 07.884′	33.60
031207–27	03.12.07	08° 46.938′	98° 08.091′	26.50
031207–29	03.12.07	08° 44.938′	98° 08.154′	25.10
031207–30	03.12.07	08° 43.714′	98° 10.957′	21.60
051207–31	05.12.07	08° 47.190′	98° 11.735′	15.80
051207–32	05.12.07	08° 46.809′	98° 11.820′	14.80
051207–33	05.12.07	08° 44.958′	98° 10.965′	17.00
051207–34	05.12.07	08° 43.000′	98° 11.916′	16.70
051207–35	05.12.07	08° 43.769′	98° 11.270′	15.20
051207–36	05.12.07	08° 43.875′	98° 10.945′	17.30
051207–37	05.12.07	08° 43.783′	98° 11.087′	17.00
051207–38	05.12.07	08° 43.682′	98° 11.168′	15.10
051207–39	05.12.07	08° 43.635′	98° 10.933′	17.50
051207–40	05.12.07	08° 43.584′	98° 10.655′	17.80
051207–41	05.12.07	08° 43.458′	98° 10.753′	16.80
051207–42	05.12.07	08° 43.319′	98° 10.908′	15.70
051207–43	05.12.07	08° 43.344′	98° 10.587′	17.70
051207–44	05.12.07	08° 43.314′	98° 10.335′	18.20
051207–45	05.12.07	08° 43.178′	98° 10.446′	17.50
051207–46	05.12.07	08° 43.040′	98° 10.639′	16.90
051207–47	05.12.07	08° 43.023′	98° 10.217′	18.30
051207–48	05.12.07	08° 42.901′	98° 09.988′	17.80
071207–49	07.12.07	08° 30.222′	97° 59.124′	62.00
071207–50	07.12.07	08° 32.753′	97° 59.865′	57.90
071207–51	07.12.07	08° 32.967′	97° 59.587′	58.60
071207–52	07.12.07	08° 33.171′	97° 59.567′	59.80
071207–53	07.12.07	08° 33.421′	97° 58.422′	59.80
071207–54	07.12.07	08° 33.804′	97° 58.674′	64.30
071207–55	07.12.07	08° 33.810′	98° 00.908′	57.10
071207-56I	07.12.07	08° 32.841′	98° 04.199′	42.90
071207-56II	07.12.07	08° 32.829′	98° 04.223′	42.90
071207–57	07.12.07	08° 31.802′	98° 04.548′	40.70
071207–61	07.12.07	08° 35.863′	98° 03.630′	45.60
071207–62	07.12.07	08° 36.320′	97° 59.492′	57.50

Table 2 (*continued*)

| Sample No.	Date	Latitude	Longitude	Water depth (m)
071207–63	07.12.07	08° 39.859′	98° 00.667′	50.70
071207–64	07.12.07	08° 39.861′	98° 00.510′	49.50
071207–65	07.12.07	08° 42.630′	98° 03.954′	40.40
071207–66	07.12.07	08° 38.759′	98° 06.205′	35.80
081207–69	08.12.07	08° 43.102′	98° 11.212′	14.20
081207–70I	08.12.07	08° 43.047′	98° 11.060′	15.00
081207–70II	08.12.07	08° 43.042′	98° 11.096′	15.10
081207–71	08.12.07	08° 42.928′	98° 10.906′	15.80
081207–72I	08.12.07	08° 42.873′	98° 10.892′	16.10
081207–72II	08.12.07	08° 42.848′	98° 10.918′	16.30
081207–73	08.12.07	08° 42.782′	98° 11.023′	14.40
081207–74	08.12.07	08° 42.744′	98° 10.866′	16.50
081207–75	08.12.07	08° 42.646′	98° 10.744′	16.80
081207–76	08.12.07	08° 42.950′	98° 11.791′	12.70
081207–77	08.12.07	08° 42.569′	98° 11.680′	13.90
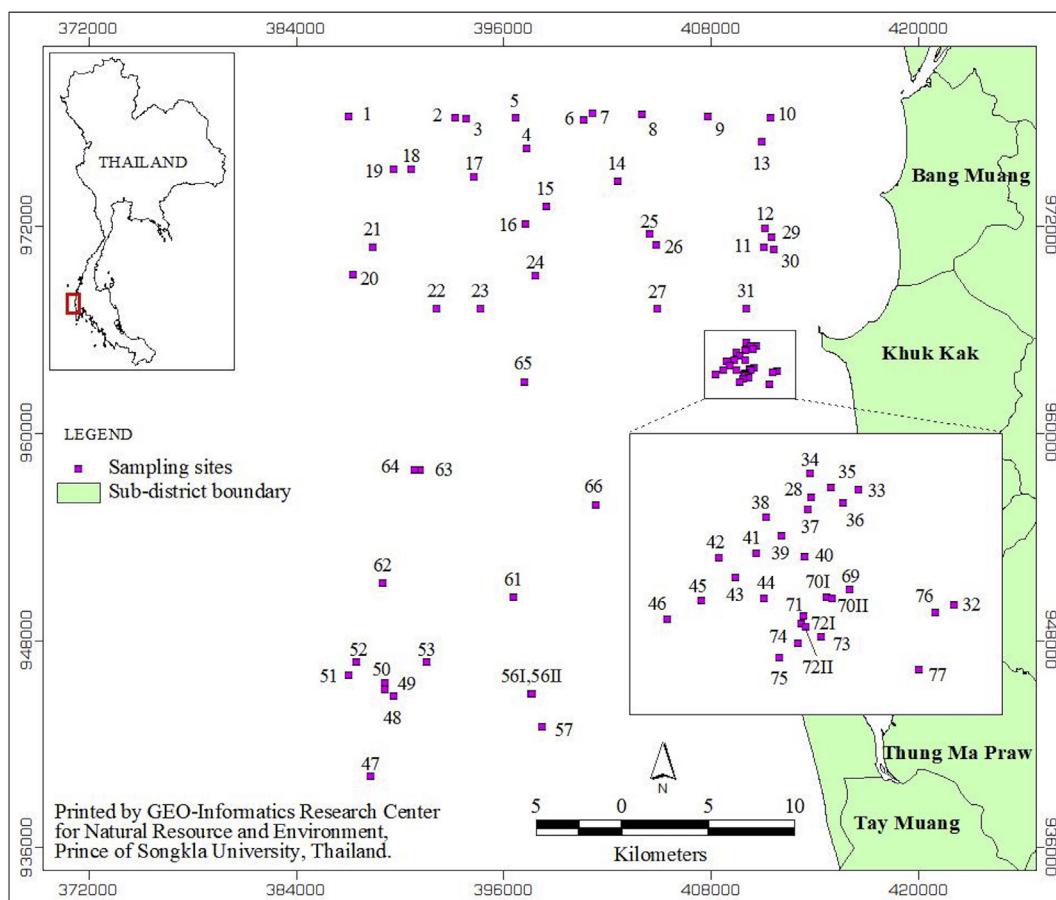
Figure 1. Sediment collecting sites at the tsunami-attacked coastal areas of Andaman Sea.

pesticides) as promising geochemical tracers to identify tsunami deposits on the coastal region around Sendai due to its higher source specificity and comparatively strong chemical structures (Bellanova et al., 2016). There are numerous benefits of using PAHs as geochemical tracers for classifying tsunami backwash deposits. Firstly, PAHs are persistent organic pollutants and thus possess a comparatively long half-life in the environment. Secondly, PAHs are hydrophobic chemical substances which describes the fact that PAHs do not combine with water molecules. Thirdly, previous studies highlight the benefits of using diagnostic binary ratios of PAHs as geochemical tracers for classifying potential emission

sources (Yunker et al., 2002, 2005, 2011; Yunker and Macdonald, 2003). A similar investigation associated with chemical characterization of PAHs in tsunami deposits were conducted at Kahana Valley, O'ahu, Hawaii, USA (Bellanova et al., 2020a). Geochemical identification of tsunami deposits indicates that organic markers can be considered as another high-resolution, multi-proxy protocol for characterizing tsunamis in the marine sediments (Bellanova et al., 2020a). It is also crucial to underline that LMW PAHs (i.e. fluoranthene, pyrene, and benzo[a] anthracene) have been detected as the most suitable organic biomarkers for historic fire events in lake sediment (Denis et al., 2012), terrestrial

Table 3. Comparisons of diagnostic binary ratios of the sediment PAHs between this study and other world sediment samples.

Reference	This study	a	b	c	d	e	f	g	h	i	j	k	l	l	l	l	m	n
Year		2014	2012	2010	2009	2014	2014	2012	2011	2013	2013	2016	2020	2020	2020	2020	2020	2020
Country	Thailand	Malaysia	China	China	China	China	China	China	China	China	China	East	Baltic	North	Bohai	Yellow	Hormozgan	Nigeria
Area	Khao Lak oastal Sediments	West Port	Liaohe Estuarine Wetland	Bohai Bay Intertidal Zone	Yellow River Estuary	Jiaozhou Bay Wetland	Guan River Estuary	Chongming Wetland	Quanzhou Bay	Baguang Wetland	Ramsar Swamp of Hongkong	Antarctica Prydz Bay	Sea	Sea	Sea	Sea	Persian Gulf	Niger Delta Bonny Estuary
Unit	$\mu g\ kg^{-1}$	$\mu g\ kg^{-1}$	$\mu g\ kg^{-1}$	$\mu g\ kg^{-1}$	$\mu g\ kg^{-1}$	$\mu g\ kg^{-1}$	$\mu g\ kg^{-1}$	$\mu g\ kg^{-1}$	$\mu g\ kg^{-1}$	$\mu g\ kg^{-1}$	$\mu g\ kg^{-1}$	$\mu g\ kg^{-1}$	$\mu g\ kg^{-1}$	$\mu g\ kg^{-1}$	$\mu g\ kg^{-1}$	$\mu g\ kg^{-1}$	$\mu g\ kg^{-1}$	$\mu g\ kg^{-1}$
$\Sigma PAHs(3,4)/\Sigma PAHs(5,6)$	1.35	2.20	3.53	24.40	2.00	2.00	0.21	2.94	1.58	2.67	1.55	3.47	1.57	1.36	1.42	1.00	2.82	0.89
$An/\Sigma 178$	0.11	0.69	0.11	0.04	0.15	0.06	0.55	0.13	0.00	0.13	0.45	0.05	0.12	0.18	0.11	0.09	0.24	0.32
$Fluo/\Sigma 202$	0.35	0.21	0.57	0.69	0.51	0.56	0.59	0.57	0.39	0.54	0.43	0.50	0.56	0.52	0.58	0.59	0.52	0.42
$B[a]A/\Sigma 228$	0.49	0.92	0.37	0.38	0.40	0.07	0.48	0.37	0.85	0.64	1.00	0.28	0.41	0.36	0.28	0.24	0.24	0.51

[a] Adapted from Sany et al. (2014).
[b] Adapted from Lang et al. (2012).
[c] Adapted from Jiao et al. (2010).
[d] Adapted from Yamei et al. (2009).
[e] Adapted from Yang et al. (2014).
[f] Adapted from He et al. (2014).
[g] Adapted from Wang et al. (2012).
[h] Adapted from Zhuang et al. (2011).
[i] Adapted from Zeng et al. (2013).
[j] Adapted from Cai et al. (2013).
[k] Adapted from Xue et al. (2016).
[l] Adapted from Wang et al. (2020).
[m] Adapted from Jahromi et al. (2020).
[n] Adapted from Anyanwu et al. (2020).

Table 4. Binary ratios of PAHs in marine sediments collected at the Khao Lak coastal sediments in comparison with numerous potential sources.

Ratios	This Study	Petroleum	Mixed Sources	Combustion		References
LMW/HMW	1.29	>1		<1	Grass, Wood and Coal	Sicre et al. (1987)
						Budzinski et al. (1997)
						Cardellicchio et al. (2007)
Phe/An	8.15	>10		<10	Grass, Wood and Coal	Baumard et al. (1998a)
Fluo/Pyr	0.54	<1		>1	Grass, Wood and Coal	Baumard et al. (1998b)
Fluo/(Fluo+Pyr)	0.35	<0.4	0.4–0.5	>0.5	Grass, Wood and Coal	Yunker et al. (2002)
An/(An+Phe)	0.11	<0.1		>0.1	Combustion	Yunker et al. (2002)
B[a]A/(B[a]A+Chry)	0.49	<0.2	0.2–0.35	>0.35	Combustion	Yunker et al. (2002)
Ind/(Ind+B[g,h,i]P)	0.34	<0.2	0.2–0.5	>0.5	Grass, Wood and Coal	Wang et al. (1999)

soils (Kim et al., 2003; Sojinu et al., 2011; Vergnoux et al., 2011), and marine deposits (Olivella et al., 2006; Stout et al., 2001; Vila-Escalé et al., 2007). Furthermore, previous studies indicate the role of volcanic dust in the atmospheric transport and deposition of PAHs (Stracquadanio et al., 2003), particularly in the aquatic ecosystem (Kozak et al., 2017). As a consequence, it appears reasonable to assume that PAHs possess high potential as organic markers to investigate the impacts of historic

Table 5. Aerosol sampling site descriptions.

Site	Source Type	Description
PSU	Urban Residential Zone	The site was situated at about 3 m above ground level in the Faculty of Environmental Management of Prince of Songkla University, and about 550 m away from the main traffic road that leads to the city center of Hat-Yai. It is important to note that PSU1 and PSU2 represent the sampling period of June (28th -30th June, 2007) and October (24th -26th October, 2007) respectively. This site is considered as an urban residential zone.
TI	Traffic	The station was located at the traffic intersection in front of the main gate of PSU. It is situated on the eastern side and approximately 2.5 km far away from the Hat-Yai city center. This station is regarded as a traffic area closed to urban residential zone. The air samples were collected on 5th – 7th July, 2007.
CI	Timber	This station is a part of Kor-Hong temple, located at the northern side and about 1.5 km far way from TI. Since timbers and tires were generally used as fuel for corpse incineration, this site is considered as an emission source of both timbers and tires-burning. This site represents the sampling period of 19th – 21st July 2007.
CPF	Crude Oil	This site was situated inside the fish can manufacturing factory of Charoen Phokphand group, which is the largest business conglomerate in Thailand. As crude oil was used for the fish can production, this station can be regarded as an emission source of crude oil-burning. The monitoring was conducted on 24th – 26th July 2007.
SL	Rural Background	This station was located at the south of Songkhla Lake and approximately 13 km far away from the northern side of PSU. This site is also situated about 14 km away from the western side of the Gulf of Thailand. Since there are not many industrial and/or traffic emission sources including chemical and metallurgy factories, power plants, and etc in this district, we consider this site as a rural background sampling station. SL1 and SL2 represent the monitoring period of July (27th – 29th July, 2007) and October (20th – 22nd October, 2007) respectively.
RMF1	Timber	This monitoring site was located at Tumbol Tungwan, Hat-Yai district. As a part of manufacturing process, the rubber sheet was treated with steam of high temperature and high pressure coupling with the purification by using sulfuric acid solution. Since Para rubber trees were used as fuel for this process, this site represents an emission of mixed Para rubber trees burning, latex fragments and sulfuric acid aerosols. The air samples were collected from 30th July to 1st August 2007.
RMF2	Timber	This station was situated at Tumbol Tachang, Banglum district. Both RMF1 and RMF2 are regarded as an emission of mixed Para rubber trees burning, latex fragments and sulfuric acid aerosols. The air samples were collected from 2nd – 4th August 207.
BT	Diesel Engine	This site was located at the south-western side of PSU and approximately 1.4 km far away from the campus. This station was selected as a source of diesel emission because the majority of these buses are diesel-fueled. The air sample collection was started from 5th – 7th August 2007.
WI	Solid Waste + Crude Oil	This site was situated at the city center and belongs to the municipality of Hat-Yai city. Since the municipal waste incinerated is a heterogeneous mixture of solid wastes and burning fuels, this site can be recognized as a combination of solid waste burning and diesel exhaust emission. The air samples were collected from 28th – 30th August, 2007.
BF	Charcoal	This site was located inside the PSU campus on the top roof of Faculty of Natural Resources. The barbeque festival has become an annual tradition that is held on the second week in August. The 40th Annual Barbecue Festival is set for Wednesday, August 15th, 2007. This site can be considered as an emission of charcoal burning. The air samples were collected from 15th – 18th August, 2007.
PR	Traffic	This station was located at the heart of Hat-Yai city. The air mass collected at this area reflected the heaviest burden from traffic congestions with the mixture of diesel and benzene exhaust emissions. The monitoring was conducted on 27th – 29th August, 2007.
KHH	Urban Background	This site was situated at the radio station on the top of Kor-Hong hill with the elevation of 356 m. The air mass passed over the station was considered as a mixture of all emission sources in urban area, and thus can be regarded as an urban residential zone monitoring site. The sampling was conducted on 3rd – 5th November, 2007.
RSB	Biomass Burning	The rice straw burning has been the major practice for removing rice straw because it is fast, economical and practical in removing disease organisms. Although the options for the disposition of rice straw are limited, this practice leads to unacceptable air pollution. The station was situated at rice field in Satingpra district, Songkhla Province and considered as a represent of biomass burning. The sampling was conducted on 16th November, 2007.
BB	Biomass Burning	As a part of soil preparation process, the biomass must be disposed of in order to make way for the plantation. The sampling site was adjacent to the unused land, and located at Namom district, Songkhla Province. This site can be regarded as an emission source of biomass burning. The sampling was conducted on 17th November, 2007.
PTB	Biomass Burning	This station is located Namom district, Songkhla Province and can be recognized as an emission source of Para rubber tree burning. The air samples were collected on 18th November, 2007.

Table 6. Diagnostic binary ratios of PAHs in Andaman marine sediments in comparison with those of particulate PAHs from other locations in Thailand.

	Khao Lak Coastal Area, Andaman Sea (Sediment Samples; n = 70; see Table 3)	Phuket (PM$_{2.5}$; n = 61; ChooChuay et al., 2020a)	Bangkok PM$_{2.5}$; n = 72; ChooChuay et al. (2020b)	Chiang-Mai PM$_{2.5}$; n = 65; ChooChuay et al. (2020c)	Various Emission Sources (PM$_{10}$; n = 17; see Tables 4 and 5)	ANOVA-Test
An/(An+Phe)	0.106 ± 0.0340	0.16 ± 0.025	0.15 ± 0.15	0.14 ± 0.10	0.130 ± 0.114	S
Fluo/(Fluo+Pyr)	0.352 ± 0.0906	0.54 ± 0.058	0.45 ± 0.47	0.52 ± 0.48	0.495 ± 0.0533	S
B[a]A/(B[a]A+Chry)	0.545 ± 0.0929	0.87 ± 0.060	0.55 ± 0.46	0.84 ± 0.65	0.508 ± 0.0983	S
B[a]P/(B[a]P+B[e]P)	0.374 ± 0.0959	0.52 ± 0.084	0.58 ± 0.59	0.55 ± 0.65	0.411 ± 0.152	S
Ind/(Ind+B[g,h,i]P)	0.293 ± 0.109	0.48 ± 0.072	0.40 ± 0.36	0.47 ± 0.50	0.455 ± 0.0744	S
B[k]F/Ind	1.04 ± 0.763	0.71 ± 0.92	0.66 ± 0.66	0.47 ± 0.52	0.217 ± 0.164	S

*S: Significant ($p < 0.05$), **NS: Non-Significant.

Table 7. Statistical descriptions of meteorological parameters and sampling positions.

Site	Site Full Name	Sampling Period	Latitude	Longitude	Average T[1] [°C]	Average RH[2] [%]	Average AP[3] [mbar]
PSU	Prince of Songkla University	28/06/07–30/06/07	7°00′21.28″N	100°29′53.27″	30 ± 3	66 ± 20	1007.8 ± 1.5
TI	Traffic Intersection	05/07/07–07/07/07	7°00′30.81″N	100°29′39.21″E	27 ± 3	79 ± 12	1008.1 ± 1.0
CI	Corpse Incinerator	19/07/07–21/07/07	7°01′17.55″N	100°29′41.44″E	32 ± 3	61 ± 13	1007.4 ± 0.6
CPF	Charoen Pokapan Factory	24/07/07–26/07/07	6°54′16.38″N	100°28′05.15″E	32 ± 1	65 ± 6	1007.8 ± 0.6
SL	Songkhla Lake	27/07/07–29/07/07	7°10′02.92″N	100°35′11.36″E	29 ± 2	68 ± 10	1006.8 ± 0.6
RMF1	Rubber Manufacturing Factory 1	30/07/07–01/08/07	7°03′19.97″N	100°37′58.90″E	30 ± 1	69 ± 9	1008.1 ± 1.0
RMF2	Rubber Manufacturing Factory 2	02/08/07–04/08/07	7°03′06.28″N	100°24′07.77″E	32 ± 1	57 ± 10	1008.8 ± 0.6
BT	Bus Terminal	05/08/07–07/08/07	6°59′42.78″N	100°28′58.02″E	33 ± 1	53 ± 3	1008.1 ± 1.0
WI	Waste Incinerator	08/08/07–10/08/08	6°57′15.43″N	100°24′00.46″E	31 ± 1	64 ± 8	1007.8 ± 0.6
BF	Barbeque Festival	15/08/07–17/08/07	7°00′23.09″N	100°30′00.54″E	32 ± 2	60 ± 2	1007.8 ± 0.6
PR	Pekrasem Road	27/08/07–29/08/07	7°00′52.99″N	100°28′20.50″E	28 ± 3	73 ± 19	1007.1 ± 2.0
KHH	Kor Hong Hill	03/11/07–05/11/07	7°00′57.92″N	100°31′12.76″E	28 ± 2	73 ± 11	1008.1 ± 0.0
RSB	Rice Straw Burning	16/11/07	7°27′00.52″N	100°25′19.02″E	31	79	1007.1
BB	Bush Burning	17/11/07	6°57′40.45″N	100°33′06.68″E	31	66	1007.1
PTB	Para Rubber Three Burning	18/11/07	6°57′40.45″N	100°33′06.68″E	27	79	1006.1

[1] T: Temperature.
[2] RH: Relative Humidity.
[3] AP: Air Pressure.

tsunami particularly in the volcanic regions and/or heavily forest-fire affected coastal sediments.

Some particular concerns with respect to the contaminations of polycyclic aromatic hydrocarbons (PAHs) and other chemical compounds in tsunami-inundated area were subsequently investigated in Phang Nga province, Thailand (Pongpiachan et al., 2013a,b,c; Pongpiachan, 2014; Prasath and Khan, 2008; Tipmanee et al., 2012). Twelve PAH congeners (i.e., phenanthrene (Phe), anthracene (An), fluoranthene (Fluo), pyrene (Pyr), benz[a]anthracene (B[a]A), chrysene (Chry), benzo[b]fluoranthene (B[b]F), benzo[k]fluoranthene (B[k]F), benzo[a]pyrene (B[a]P), indeno[1,2,3-cd]pyrene (Ind), dibenz[a,h]anthracene (D[a,h]A), and benzo[g,h,i]perylene (B[g,h]P) were comprehensively characterized in marine deposits at the 26 December 2004 Indian Ocean tsunami affected coastal area (Pongpiachan et al., 2013a). According to the report, ∑12PAHs in this study were remarkably under other values detected in coastal deposits around the world. In spite of comparatively low ∑12PAH contents detected in the tsunami-inundated zone, some unique accomplishments are worthy enough to be discussed. Further efforts towards the application of chemical proxy to clarify the sediment transport mechanism triggered by successive tsunami run-up and back wash phenomena had been conducted by analysing PAH congeners in coastal deposits coupled with the employment of several multivariate descriptive statistical techniques (Tipmanee et al., 2012). Some other levels of efforts to elucidate the depositional processes after tsunami back wash phenomena were made by comprehensively characterize the spectrum of functional groups in tsunami sediments by using Fourier

Transform Infrared (FTIR) and micro-beam synchrotron X-ray fluorescence (μ-SXRF) (Pongpiachan et al., 2013b,c).

Recognizing the processes and spatial distributions of tsunami inundation and sediment transport needs some innovative concepts to distinguish between terrigenous and marine deposits of aromatic compounds. Besides, the role of the continental shelf as an emission source of aromatic compounds should theoretically be discriminated from those of sea floors, as sink areas and the combination between the two should also be carefully investigated. Numerous techniques have been applied to discriminate between marine and terrigenous components in coastal deposits by aromatic compounds such as PAHs, hopanes and cholestanes (e.g. 17 α(H) -22,29,30-Tris (Tm), 17 β(H), 21 β (H) -hopane, 17 β (H), 21 α (H) -30-northpane (Isoadiatane), 17 β (H), 21 α (H) -hopane (Moretane), 17 α (H), 21 β (H) –hopane, 18 α (H), 22,29,30-Trisnorneohopane (Ts)) (Westerholm et al., 1992; Yunker et al., 2002; Yunker and Macdonald, 2003; Kalaitzoglou et al., 2004). By computing aromatic compound contents against natural background concentrations, the geographical expansion of tsunami backwash deposits can roughly be evaluated.

There are several benefits to use aromatic compounds as chemical tracers. Firstly, aromatic compounds have some preferences that they are both intentionally and unintentionally emitted into the environment by incomplete ignitions of fossil fuels and biomasses and hence can be employed as tracers to characterize anthropogenic ignition origins (e.g. vehicular exhausts, power plants, factories etc) from natural burning sources (e.g. biomass burnings, agricultural waste burnings, and volcano

Table 8. Principal component analysis of PAHs in marine sediments.

PAH Congeners	Principal Component (PC)				
	PC 1	PC 2	PC 3	PC 4	PC 5
Phe	0.031	0.080	**0.943**	0.234	-0.058
An	0.174	0.040	**0.927**	0.262	-0.111
Fluo	0.070	0.385	-0.191	**0.592**	**0.592**
Pyr	-0.029	0.011	-0.076	0.171	**0.973**
B[a]A	-0.091	-0.150	0.390	**0.867**	0.151
Chry	-0.065	-0.148	0.360	**0.893**	0.143
B[b]F	**0.880**	0.233	0.360	0.045	-0.054
B[k]F	**0.846**	0.210	-0.018	-0.252	0.088
B[e]P	**0.973**	0.011	-0.042	0.037	-0.059
B[a]P	**0.833**	0.486	0.111	0.004	0.031
Ind	**0.842**	0.483	0.018	-0.009	-0.015
D[a,h]A	0.299	**0.913**	0.038	-0.092	0.098
B[g,h,i]P	0.384	**0.889**	0.086	-0.105	0.015
Initial Eigenvalues Total of Variance (%)	41.80 %	24.90 %	15.17 %	8.69 %	3.80 %
Probable Source Type	Biomass	Wood	Diesel	Oil	Fugitive
	Burning	Combustion	Emission	Combustion	Emission

Bold represents the value of correlation coefficient larger than 0.5.

activities) by adopting certain diagnostic binary ratios (Pongpiachan, 2013a,b,c; Pongpiachan et al., 2013d,e; Tipmanee et al., 2012; Yunker et al., 2002). Secondly, PAHs has generally long atmospheric lifetime as a consequence of its comparatively strong aromatic ring structure (Pongpiachan, 2010). Earlier studies have also revealed that OH radicals are the most reactive oxidant for PAHs, followed by NO_3 and O_3 (Atkinson and Arey, 1994; Atkinson and Aschmann, 1987). Since PAHs are generally well-preserved in marine sediments with strictly limited level of lighting, it appears reasonable to assume that photodecomposition, heterogeneous and homogeneous reactions are not the main sinks of PAHs. Thirdly, PAHs has extremely low aqueous solubility due to its relatively high hydrophobicity in comparison with other organic compounds. As a consequence, it seems rationale to conclude that PAHs can be considered as alternative chemical tracer for investigating tsunami backwash deposits.

Overall, the principle aims of this manuscript is to provide contextual information and state-of-the-art of applying PAHs coupled with FTIR and μ-SXRF to discriminate tsunami backwash deposits from typical marine sediments. One of the main success key factors in tsunami mitigation strategies is to identify historic tsunami deposits which relies on the advancement of applying numerous analytical techniques. This manuscript is unique because it contains detailed information of analytical methods of chemical tracers as well as applications of advanced statistical techniques to characterize tsunami backwash deposits.

1.2. General hypothesis

After achieving its maximum run-up height, the backwash phenomenon took place and resulting for channelized and erosions in certain areas. As a consequence, it is most probably that offshore tsunami backwash deposits possess both crustal components and re-deposited maritime sediments. Previous studies have shown that tsunami backwash deposits contained suspended material, while deposits caused by runoff following monsoon/cyclone/storm are generated by bed load transport (Dawson and Shi, 2000; Dawson and Stewart, 2007; Yoshii et al., 2018). Based on the assumption of non-extreme event conditions, it appears rationale to consider that terrestrial debris may be transferred to the marine floor as well. This normal condition will theoretically consume relatively longer time than the "tsunami backwash phenomenon", and thus the "crustal set of PAH distinctive patterns" might be hypothetically recorded. While previous investigations have assumed

that deposits detected farther inland than the possible inundation limit of storm surges were tsunami deposits, a recent study related with tsunami and storm events on the Sendai Plain, Japan highlighted that the coastal topography also plays an important role in governing inundation distances of both tsunami and storm deposits (Watanabe et al., 2018). It is also crucial to underline that topographic features played a crucial role in onshore sediment transport (Sugawara et al., 2014). In these unique situations, two categories of hypothesis can be proposed. Please note that these ideas are merely speculative but that no data are provided to prove it is true or not.

Hypothesis I. (Dissimilarity in transportation process)

It seems reasonable to assume that different molecular weight of PAH congeners present in different particulate sizes (Kukkonen and Landrum, 1996; Wang et al., 2001). It is well known that PAHs tend to rather to be adsorbed to organic matter (e.g. black carbon), which is more common in fine sediments rather than to just sediment (e.g. sand) of different sizes (Cornelissen et al., 2005; Lohmann et al., 2005). It is also crucial to underline that sediment of different sizes possess various organic matter contents (Christensen, 1992; Kukkonen and Landrum, 1996.). Since tsunami waves can transfer all particle sizes of terrigenous debris, it is therefore most probably that tsunami backwash debris will possess a different "distribution pattern of PAHs" in comparison with those of monsoon originated deposits.

Hypothesis II. (Dissimilarity in erosion period)

While tsunami backwash took place in comparatively fast within time scale of minutes, the flooding of monsoon extended for numerous hours. Dissimilarities in the "inundation period" responsible for the fractionization of PAH congeners as a consequence of its dissimilarities under the context of "water solubility". For example, Phe is relatively more hydrophilic than B[a]P (Lu et al., 2008). In the case of prolonged inundation, the greater quantity of Phe will naturally dissolve into backwash water in comparison with B[a]P. Generally, n-octanol/water partition coefficients (K_{ow}) have been widely used as indicators for evaluating aqueous solubilities of PAHs (de Maagd et al., 1998; Kamlet et al., 1988; May et al., 1978). The log K_{ow} values for PAHs ranged from 3.32 (Naph) to 6.30 (Ind) (Sahu and Pandit, 2003). It is well known that the aqueous solubility of PAHs is negatively correlated with its molecular weight. Hence, the monsoon originated sediments will theoretically possess Phe more than B[a]P. On the contrary, this unique phenomenon will not occur in the case of tsunami backwash deposit. Since the tsunami wave
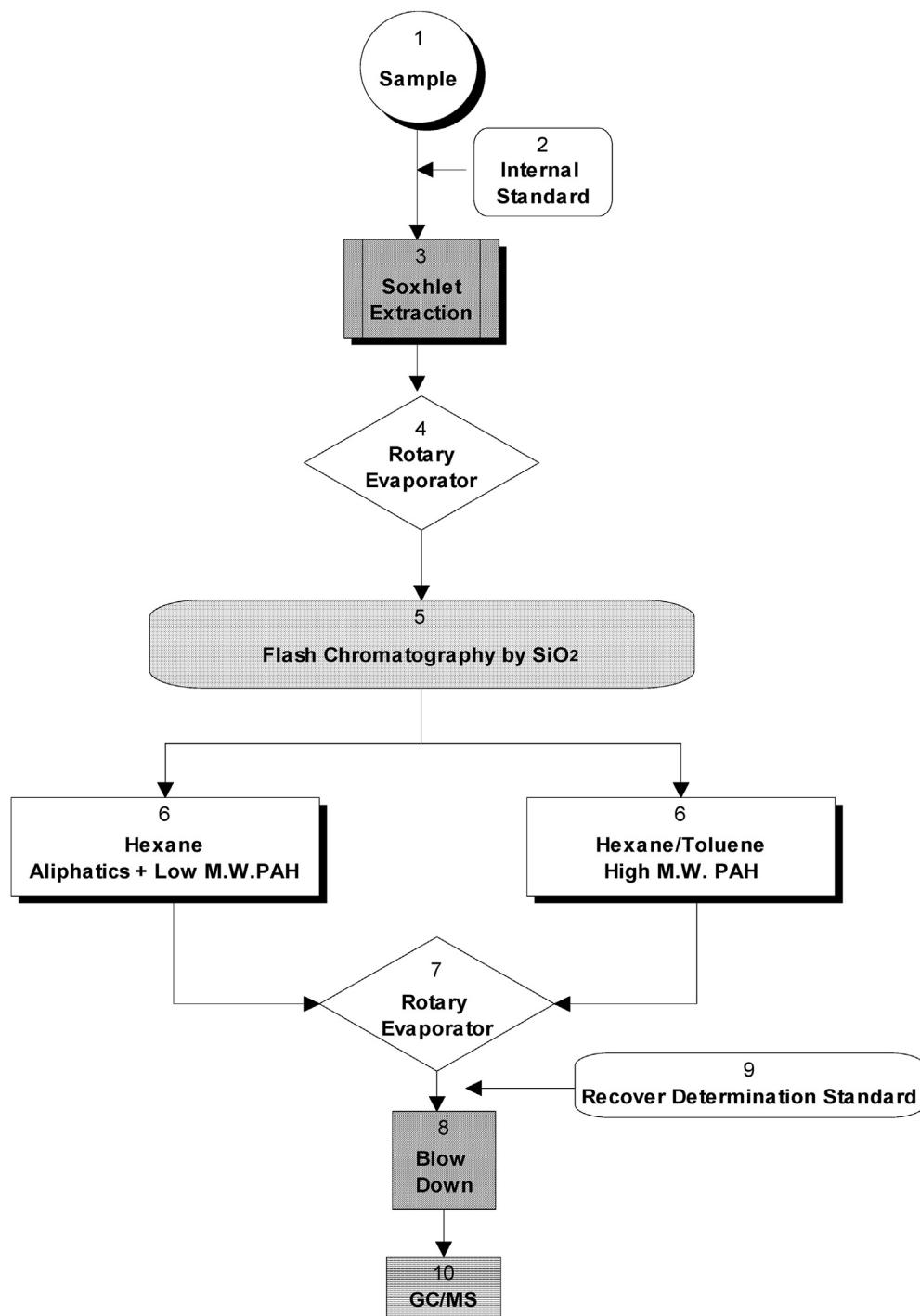
Figure 2. Scheme of fractionation using the flash chromatography method.

occur comparatively in short time scale of minutes, both LMW PAHs (e.g. Phe) and HMW PAHs (e.g. B[a]P) will hypothetically be transferred into sea floor by tsunami wave simultaneously without giving any time for the fractionization effect. However, it is crucial to underline that this hypothesis cannot be applied to all cases. For instance, the first results of a geological survey following the 2011 Tohoku-oki tsunami found some brackish ponded water on land and still recorded seven months after tsunami (Chagué-Goff et al., 2012, 2014; Goto et al., 2011).

The concept of source profile represents the unique chemical information of several potential sources of the marine deposits obtained at any receptor sites. Since diagnostic binary ratios of two or three PAH congeners are still vulnerable to both photo-decomposition, homogeneous/ heterogeneous reaction coupled with microbiological degradation and thus may be not sufficient enough to categorize PAH emission sources at any fixed observatory sites. One of more appropriate strategies is to
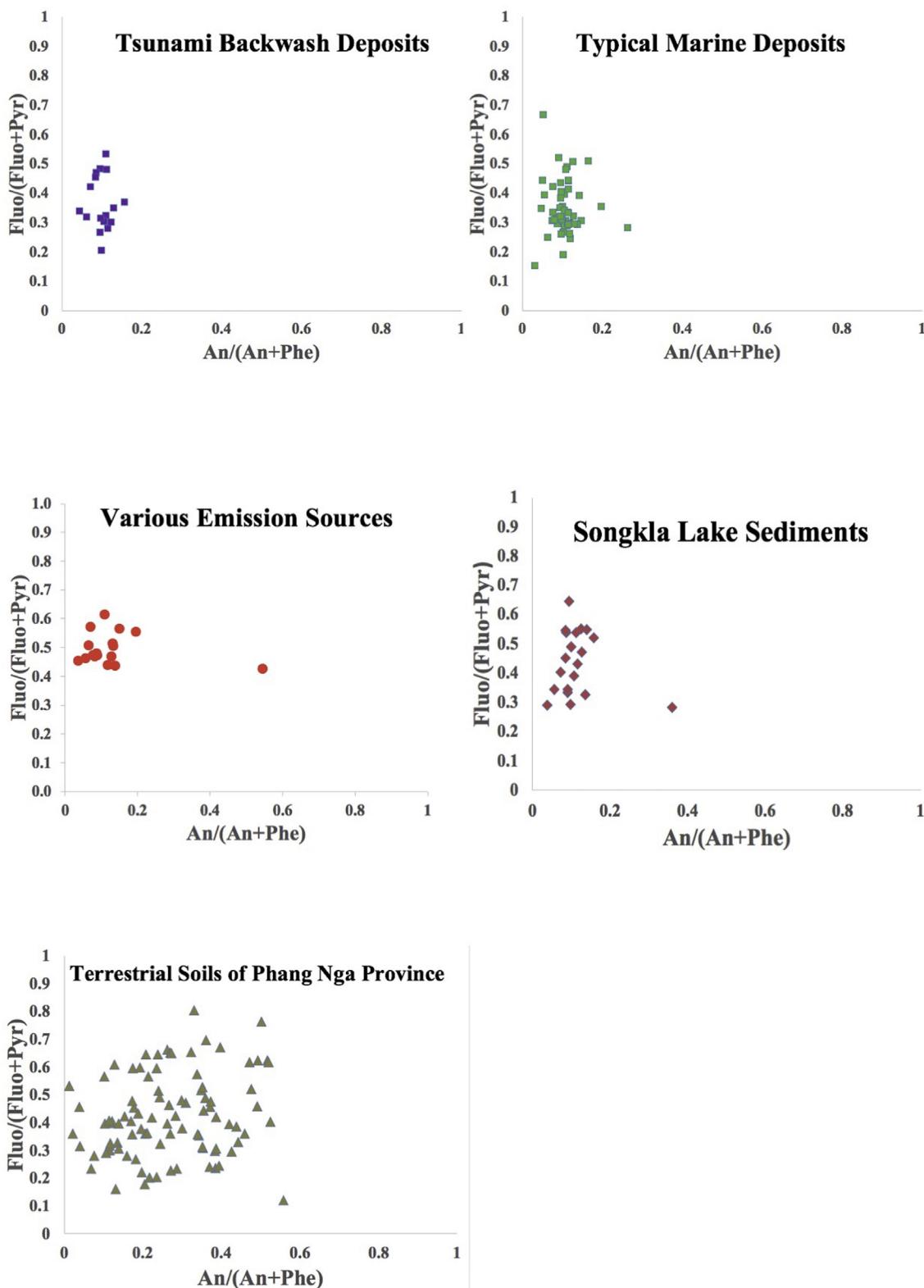
Figure 3. Diagnostic binary ratios of PAHs (i.e. Fluo/(Fluo+Pyr), An/(An+Phe)) in Tsunami backwash deposits, typical marine deposits, various emission sources, Songkla Lake sediments, and Terrestrial soils of Phang Nga Province.
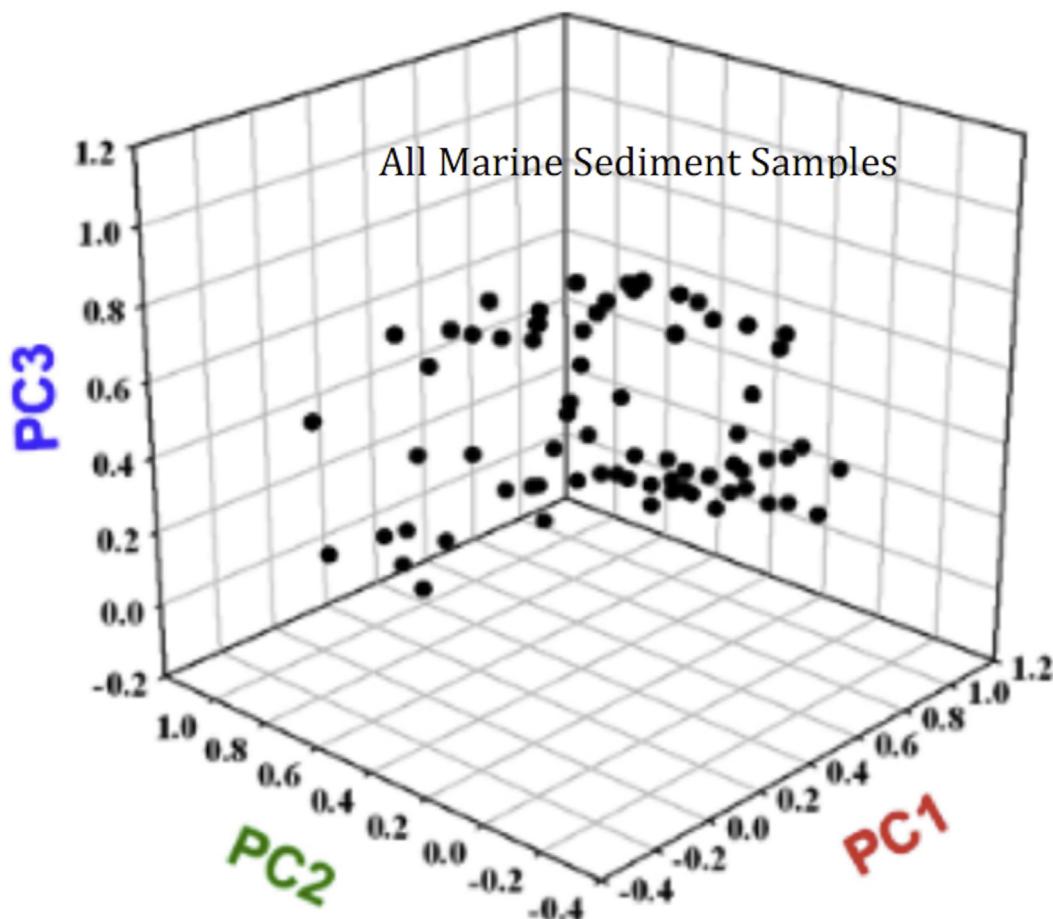
Figure 4. Three dimensional plots of PCA using PAH contents in all marine sediment samples collected in Andaman Sea.

evaluate the influence of backwash tsunami wave with the application of the overall PAH fingerprints.

2. Physico-chemical properties and degradation mechanisms of PAHs

2.1. Physico-chemical properties

PAH congeners are a group of comparatively persistent organic compounds consist of only carbon and hydrogen and comprise two (e.g. naphthalene) to eight benzene rings (e.g. phenanthro-5,4,3,2-[e,f,g,h,i] perylene) (see Table 1). There is a large variation in vapour pressure of subcooled liquid of PAH congeners starting from 9.16×10^{-8} atm (i.e. D [a,h]A) to 4.14 atm. Similarly, Henry Law's constants range from 3.00×10^{-3} (i.e. Per) to 12.2 (Ace). A previous study highlighted the importance of water temperature as a major factor influencing water solubility of An, Pyr, Chry, and Per at temperatures ranging from 298 K to 498 K and pressures from 30 bar to 60 bar in subcritical (superheated) water while pressure had a minimal impacts (Miller et al., 1998). Enhancing water temperature up to 498 K can significantly elevated water solubilities by five orders of magnitude. For example, increasing the temperature from 298 K to 498 K increased the mole fraction solubility of chrysene from $(0.63 \pm 0.08) \times 10^{-9}$ to $(75\,800 \pm 4000) \times 10^{-9}$ (Miller et al., 1998). It is also worth mentioning that the apparent water solubility of PAHs can be increased in the presence of humic substances (Pongpiachan, 2009; Tanaka et al., 1997). Structural and compositional variations of humic and fulvic acids can play a major role on water solubility of PAHs (Chiou

et al., 1986; Gauthier et al., 1987). Significant water solubility enhancement of other POPs such as p,p'-DDT, 2,4,5,2′,5′-PCB, 2,4,4′-PCB, 1,2,3-trichlorobenzene, and lindane under the presence of dissolved humic and fulvic acids from soil and aquatic origins were previously reported (Chiou et al., 1986).

2.2. Degradation mechanisms of PAHs

2.2.1. Chemical reaction with OH radical

Multiple mechanisms are responsible for degradations of PAHs in different environmental compartments. It is crucial to note that the atmospheric lifetime, τ [s], of PAH congeners with respect to photolysis triggered by trace gaseous species such as OH, O_3 and NO_3 radicals influences the kinetics of tropospheric photochemistry of SVOCs in both vapour and aerosols. Previous studies in chamber experiments have underlined that OH radicals are the most influential oxidant for PAHs, followed by NO_3 and O_3 (Kamens et al., 1985, 1988, 1990, 1994). Aromatic compounds typically react immediately with OH radicals so that the general atmospheric lifetimes of PAHs are in the range of hours to days (Calvert et al., 2002). Although NO_3 radicals govern night-time homogeneous and heterogeneous reactions of PAHs, it is also crucial to highlight that certain PAHs have different photolysis rate constants and thus responsible for various atmospheric lifetimes. In general, the relationship between atmospheric lifetime of PAHs and other trace gaseous contents can be described as follows. Firstly, the predictions of τ were computed based on the formula.
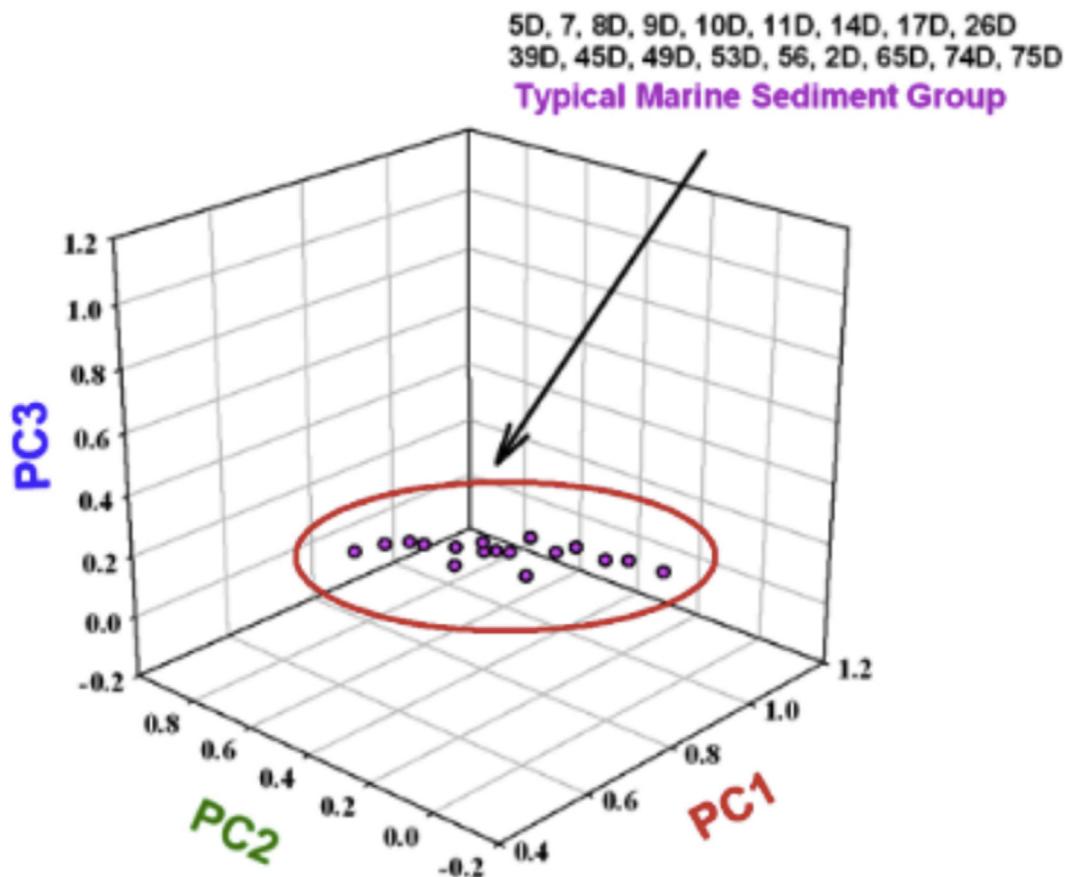
Figure 5. Three dimensional plots of PCA using PAH contents in typical marine sediment samples.

Life time estimations were calculated based on the equation recommended by Millet et al. (2004) (Eq.1)

$$\tau = \frac{1}{K_{OH}[OH] + K_{O_3}[O_3] + J} \qquad \text{Equation 1}$$

Where K_{OH} and K_{O_3} are the rate constants (dimensionless) for the reaction with OH and O_3 (Sander, 2000), and J is the photolysis rate (dimensionless). The OH concentration [molec cm^{-3}] can be calculated from the seasonal cycle equation (Eq.2):

$$[OH] = 7 \times 10^5 \left[1 - \beta \cos\left(\frac{2\pi d}{365}\right) \right] \qquad \text{Equation 2}$$

In this study, OH, d, and β stand for OH radical concentration [molec cm^{-3}], sampling interval represented in days, and a dimensionless adjustable factor, respectively. It is also crucial to note that the value of 7×10^5 molec cm^{-3} is representative of the annual mean OH concentrations in northern mid-latitude (Goldstein et al., 1995; Spivakovsky et al., 1990). When attempting to estimate the atmospheric lifetime for PAHs by applying the Millet equation, there is a crucial assumption to bear in mind that PAH content gradients are principally influenced by both heterogeneous and homogeneous chemical reactions rather than emission source variability and mixing. For most of site specific conditions, the majority of air quality observatory sites are tend to be governed by air masses of various emission sources and ages. This indicates that great care should be taken when pursuing further to elucidate the mechanisms governing chemical lifetime of PAH congeners.

2.2.2. Impacts of meteorological parameters on photo-decomposition

On the contrary, it has been reported that the initial photo-induced loss of PAHs on airborne wood soot particles can be predicted from an expression that is first order in PAHs (Kamens et al., 1985; Fan et al., 1996; Cimberle et al., 1983). This has made it possible to compute pseudo-first-order decay constants of particulate PAHs at a given solar intensity, humidity, and temperature. Kamens et al. (1988) computed the first order rate constants of eight species of high MW PAHs as a function of humidity, solar intensity and temperature by using Multiple Regression Analysis (Eq.3):

$$\ln k = const + a_1\left(\frac{1}{T}\right) + a_2 \ln I + a_3 \ln[H_2O] \qquad \text{Equation 3}$$

Where k, $const$, T, I and H_2O are a first order decay rate constant (dimensionless), constant (dimensionless), temperature (°C), solar intensity (W m^{-2}) and absolute humidity (g m^{-3}) respectively. In addition a_1, a_2, a_3 are coefficients (dimensionless) of temperature, light and water vapour in that order.

In the tropospheric atmosphere, the main degradation mechanisms for those three-ring-PAHs is considered to be by vapour-phase homogeneous reaction with OH radicals (Atkinson and Arey, 1994; Atkinson and Aschmann, 1987). Previous investigations underlined that an atmospheric lifetime of Ph and MePh group can be predicted by applying only first-order OH radical reaction rate constants (Lee et al., 2003). Since the chemical reactions between PAH congeners and NO$_3$ radicals coupled with O$_3$ are generally too slow to be of importance (Ellis et al., 2003), it seems rationale to assume that the direct photodecomposition is insufficiently rapid to affect loss rates and it is the homogeneous reactions with OH radical, which is presumably to be crucial. On the basis of the computed atmospheric lifetimes of Ac, Ace, Ph and MePh congener with respect to OH radical homogeneous reaction, significant decomposition of these LMW PAHs should take place on a numerous hour timescale, depending on the specific OH radical reaction rate constants. In addition, the comparative susceptibilities of 11 PAH congeners in solution to

2, 3D, 4D, 6D, 12AD, 12bD, 15C, 16, 18, 19D, 20D, 21D
22D, 23D, 24D, 25D, 27, 29D, 30D, 37D, 40D, 43D, 46D, 47B
48D, 50D, 51D, 52D, 55D, 56D, 57D, 61D, 62D, 63D, 64D, 66D
70_2D, 76D, 77D

**Mixture Between Typical Marine Sediemnts and Tsunami Deposits**
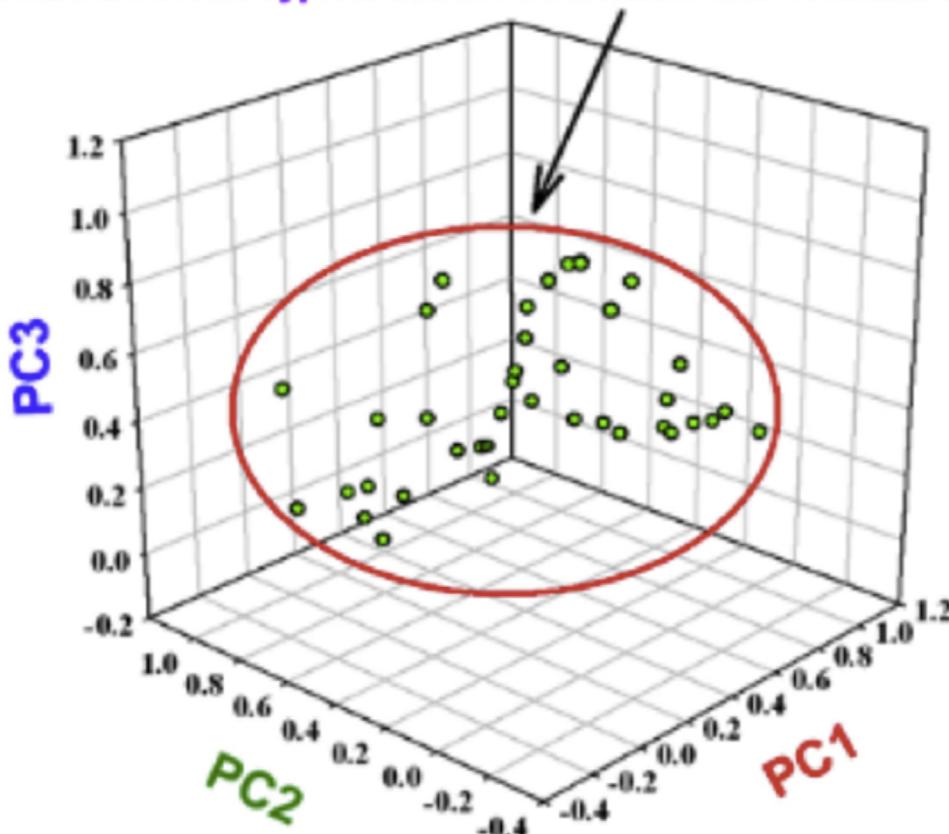
Figure 6. Three dimensional plots of PCA using PAH contents in mixture between typical marine sediments and tsunami deposits.

photodegradation under artificial sunlight were previously investigated (Sanders et al., 1993). Detected aquatic half-lives ranged by a factor of 25, from <2 h for An to 50 h for Fluo (Sanders et al., 1993).

Over the past few years, numerous studies have concentrated on the elucidations of microbiological degradation mechanisms of PAH congeners (Cerniglia, 1993). It is well known that bioremediation methods have been applied to clean up PAH contaminated terrestrial soils and sediments. As a consequence, some exceptional improvements and/or clarification of the metabolism, enzyme mechanisms, and genetics of polycyclic aromatic hydrocarbon degrading microorganisms is extremely crucial for the optimization of these bioremediation processes. Based on the literature reviews, which subsequently summarized by Cerniglia and Heitkamp (1989), some typical statements associated with the microbial degradation of PAHs can be described as follows:

(i) There are many species of bacteria, fungi, and algae that possess the capability to metabolize PAH congeners.
(ii) Hydroxylation of unsubstituted PAH congeners perpetually involves the incorporation of molecular oxygen.
(iii) High molecular weight (HMW) PAHs (i.e. > 3 rings) do not act as substrates for microbial growth, and thus they may be subject to cometabolic transformations.
(iv) LMW PAHs decay immediately, whereas HMW PAHs are comparatively persistent to microbial attack.

(v) Most instant microbial decay of PAH congeners take place at the water/sediment interface and decay rates can be largely governed by numerous aquatic conditions (e.g. pH, conductivity).

3. Research methodology

3.1. Study sites and sampling methods

Situated on the eastern coastal area of the Andaman Sea, the nearshore of Kho Lak coastal zone, Phang Nga Province, Thailand was deliberately selected as an investigation site due to severe impacts caused by tsunami waves, which flooded along a coast up to more than one kilometer inland. Numerous previous studies reported the tsunami inundation distance ranged from less than 3 km on Kho Khao Island to approximately 10 km at the Nham Kem and the Pakarang Cape (Szczuciński, 2012), coupled with the tsunami wave height reached over 15 m at the Nham Kem (Tsuji et al., 2006) and the Pakarang Cape (Siripong, 2006). The marine deposit samples were obtained in the research area covering roughly 750 km^2 (See Table 2). Andaman sea floor topography was intensively investigated with some assistances of Multibeam, Side Scan Sonar and a Boomer system for characterizing tsunami backwash sedimentary features at the target locations. All sampling sites were chosen on the basis of the data obtained from above mentioned hydro-acoustic mapping instruments (Feldens et al., 2009). Surface

31A, 32, 32D, 34D, 35D, 36D, 41D, 42C, 44D
69D, 70D, 71D, 72-2D, 72bD, 73D
**TSUNAMI DEPOSIT GROUP**
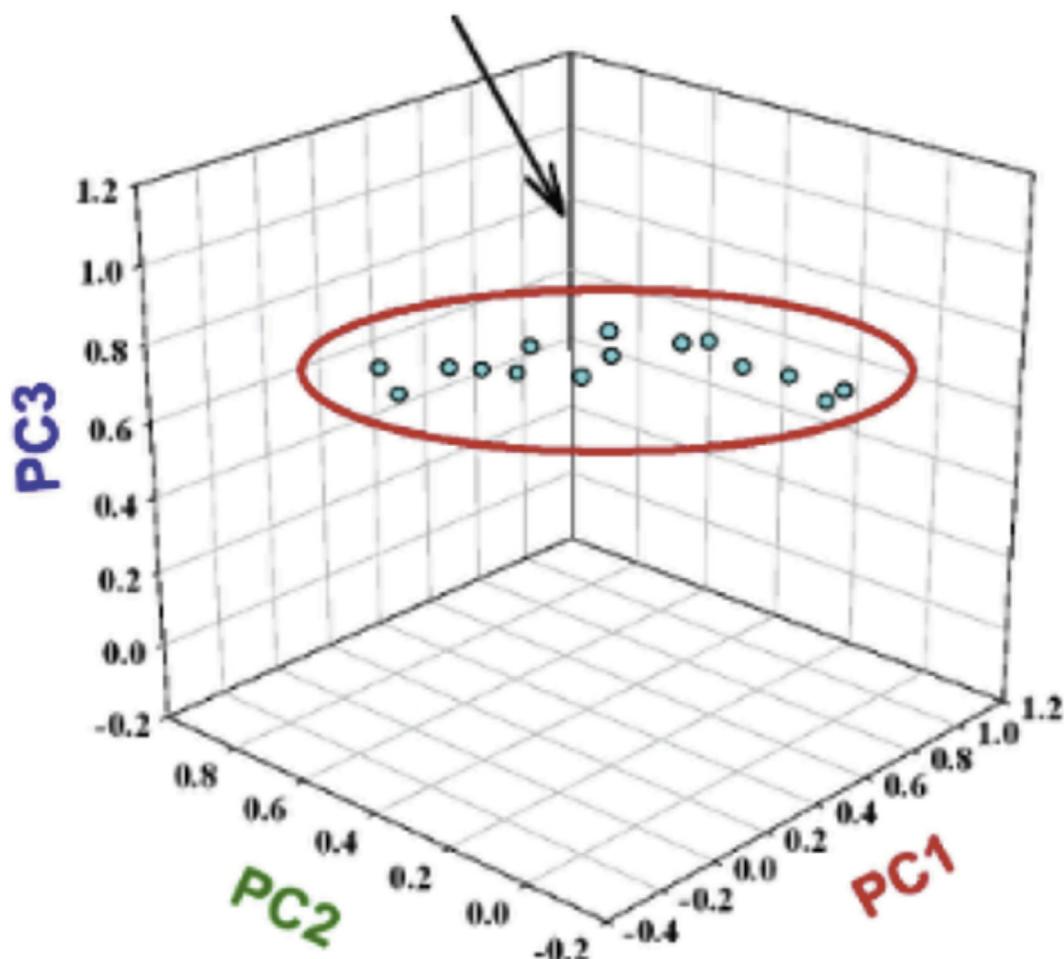
Figure 7. Three dimensional plots of PCA using PAH contents in tsunami deposit samples.

marine deposits were obtained along the Khao Lak coastal area in order to chemically characterize the distributional pattern of 13 PAH congeners namely Phe, An, Fluo, Pyr, B[a]A, Chry, B[b]F, B[k]F, B[e]P, B[a]P, Ind, D[a,h]A, and B[g,h,i]P (Pongpiachan, 2014; Tipmanee et al., 2012). In addition, the sediment sampling locations are clearly shown in Figure 1. The Van Veen Grab Sampler was employed to gather the 70 surface marine deposits during the period from 1st to 8th of December, 2007. All collected marine deposits were delicately covered in pre-cleaned aluminum foil, preserved in a glass bottle, and kept frozen at $-20\,^\circ$C. Collected sediments were freeze-dried prior to being grounded and sieved to homogenize the samples, and subsequently preserved in the cooler at $-4\,^\circ$C until chemical characterization.

3.2. Principal component analysis (PCA)

Over the past few decades, PCA has been widely used for classifying the potential sources of PAHs in numerous environmental samples completed by a rotation technique (Liu et al., 2009; Simcik et al., 1999; Tipmanee et al., 2012). For instance, PCA was successfully identified five major potential sources of PM$_{2.5}$ in ambient air of Bangkok, which were traffic emissions (44%), agricultural waste combustions (24%), maritime

aerosols (11%), electric power plants (6.5%), and manufacturing sectors (4.5%) (ChooChuay et al., 2020b). The other two comparative studies with the assistance of PCA also highlight the importance of vehicle exhausts as the most crucial source of PM$_{2.5}$ collected in ambient air of Chiang-Mai and Phuket, Thailand (ChooChuay et al., 2020a,c). PCA was also applied for source apportionment of PAHs in coastal soils collected around Koh Samed Island after the 2013 Rayong oil spill incidence (Pongpiachan et al., 2018). Similar studies were also employed PCA for quantitative analysis of potential sources of PAHs in terrestrial soils of Antarctica, Chile and Pakistan (Deelaman et al., 2020; Pongpiachan et al., 2020). In the current study, 13 parameters and 70 marine sediment samples were taken into accounts for computing PCA. Varimax rotated factor analysis was chosen for conducting PCA. In addition, all statistical analysis was carried out using the software "SPSS version 13".

4. Chemical extraction and instrumental analysis of aromatic compounds

A cocktail of 13-PAHs Norwegian Standard (NS 9815: S-4008-100-T) are carefully detected in this study. These include Phe, An, Fluo, Pyr, B[a] A, Chry, B[b]F, B[k]F, B[e]P, B[a]P, Ind, D[a,h]A, and B[g,h,i]P. The

exceedingly low quantify of PAHs in marine sediments request their enrichment chemical extraction and interference removal prior to their both qualitative and quantitative computation on a Shimadzu GCMS-QP2010 Ultra system comprising a high-speed performance system with ASSP function. More detailed GC/MS analytical protocol was mentioned in previous publications and will not be explained here (Pongpiachan et al., 2009, 2011). The analytical method used in this study and associated technical details have been discussed in our previous articles and will not be described here (Pongpiachan, 2013a,b,c; Pongpiachan et al., 2013d,e; Tipmanee et al., 2012). Briefly, the solvent extraction of PAH congeners is conducted by applying HPLC grade of dichloromethane (DCM) purchased from Fisher Scientific. It is also crucial to underline that all the Soxhlet extraction, and the fractionation/clean up processes of PAH congeners were carried on based on the protocol (Gogou et al., 1996, 1998). Standard reference material (SRM-NIST1941b-Marine Sediment) was applied to conduct both quality control and quality assurance (QC/QA) of target compounds. Average recoveries, which are fundamentally relied on chemical extraction of matrix-matched certified SRM-NIST1941b-Marine Sediment, ($n = 8$) was in range of 78–107%. In addition, the analytical precision of the protocol, which can be computed as relative standard deviation on the duplicate samples, was less than 15%.

5. Application of PAHs as geochemical tracers to characterize tsunami backwash deposits

5.1. Application of diagnostic binary ratios

As previously mentioned, PAH congeners can be emitted into different environmental compartments from both anthropogenic and natural emissions. Over the past few decades, several molecular diagnostic binary ratios of PAH congeners have been applied as geochemical tracers to classify its probable origins (Yunker et al., 2002, 2005, 2011; Yunker and Macdonald, 2003). For instance, Fluo/(Fluo+Pyr), B[e]P/(B[e]P+B[a]P), B[b,j,k]F/B[g,h,i]P, Ind/B[g,h,i]P, B[a]P/B[e]P, B[a]A/Chry, B[a]P/B[g,h,i]P and Ind/(Ind+B[g,h,i]P), have been employed as distinctive binary ratios to discriminate their potential origins for many decades (Tsapakis and Stephanou, 2005; Yunker and Macdonald, 2003). In particular, diagnostic binary ratios of Fluo/(Fluo+Pyr) and Ind/(Ind+B[g,h,i]P) were comprehensively applied as geochemical tracers to distinguish fossil combustions from other agricultural waste burnings and/or forest fires, with comparatively low ratios (i.e. <0.40 and <0.20, respectively) highlighting petrogenic source, intermediate ratios (i.e. 0.40–0.50 and 0.20–0.50) underlining vehicular exhausts, whereas values greater than 0.50 can be interpreted as indications of wood or coal combustion (Yunker and Macdonald, 2003).

In spite of its popularity as a part of source apportionment techniques, numerous concerns on applications of diagnostic binary ratios of PAH congeners were critically reviewed by Galarneau (2008). Diagnostic binary ratios of PAH congeners display considerable intra-source variability and inter-source similarity, particularly with the source identifications of aerosols. For instance, the diagnostic binary ratios of B[a]A/(B[a]A+Chry) obtained from coal combustion ranged from 0.18 to 0.49 while those of oil combustion varied from 0.12 to 0.44 (Yunker et al., 2002). The behaviour, transport and reduction of PAH congeners by wet and dry deposition phenomenon are considerably affected by the gas-particle partitioning and thus comparative PAH congeners are not well preserved in the ambient air (Birgül et al., 2011; Junge, 1977; Ollivon et al., 2002).

5.2. Impacts of gas-particle partitioning on diagnostic binary ratios of PAHs

During the early stages of gas-particle partitioning investigations, the following formula has predominantly been employed for the estimation using adsorption theory connecting the fraction on particles (ϕ) to the vapour pressure of the solid substance (P_S°) (N m^{-2}), the particle's surface (θ) (m^2), and a constant (c) (dimensionless) (Junge, 1977) (Eq.4):

$$\phi = \frac{c\theta}{(p_S^\circ + c\theta)} \qquad \text{Equation 4}$$

To assess the comparative significance of Junge *ad*sorption model (Eq.5), the estimated particulate fraction ϕ can be computed as

$$\phi = \frac{K_p TSP}{(K_p TSP + 1)} \qquad \text{Equation 5}$$

When the gas-particle partitioning is overwhelmed by *ad*sorption, K_p can be displayed by (Eq.6):

$$K_p = \frac{C_p}{C_g TSP} = \frac{N_s a_{TSP} T e^{(Q_l - Q_v)/RT}}{16 P_L^\circ} \qquad \text{Equation 6}$$

where C_p and C_g are the gas and particle phase concentrations (ng m^{-3}). N_s is the number of *ad*sorption sites (sites cm^{-2}), a_{TSP} is the surface area of TSP (m^2 g^{-1}), T is the temperature (K), R is the universal gas constant (8.3 10^{-3} kJ K^{-1} mol^{-1}), Q_l and Q_v are the enthalpies of *de*sorption and volatilisation (kJ mol^{-1}), respectively, and P_L° is the compounds' sub-cooled liquid vapour pressure (Torr). P_L° can be calculated by applying various protocols, and furthermore, many of the variables (e.g. N_s, a_{TSP}, Q_l and Q_v) are unascertained for fine particles. As a consequence, it appears problematic to obtain an actual K_p prediction based on Eq.17. On the contrary, log K_p–log P_L° correlations displayed steadily preferable regression outcomes than those applying P_S°(Eq.7):

$$Log K_p = m_r Log P_L^\circ + b_r \qquad \text{Equation 7}$$

Depended on logical examinations and empirical data from previous publications, gas-particle partitioning of PAHs (K_p) can be investigated by using Eq. 18 as a function of P_L° including both *ad*sorptive and *ab*sorptive partitioning processes. Based on Eq.18, m_r and b_r are experimental values, in spite of the partitioning phenomena. For equilibrium gas-particle partitioning, m_r is expected to have a value close to -1 (Pankow, 1994). Finizio et al (1997)(2021) reported an equation to estimate K_p values of PAHs by applying only octanol/air partition coefficient (K_{OA}) assuming that *ab*sorption is the major sorption phenomena (Eq.8).

$$K_P = f_{OM} \frac{MW_{oct}\gamma_{oct}}{MW_{OM}\gamma_{OM}10^9\rho_{oct}} K_{oa} \qquad \text{Equation 8}$$

Where ρ_{oct}(820 kg m^{-3} at 20 °C) is the density of the octanol and γ are the activity coefficients of the PAHs in OM ($_{OM}$) and octanol ($_{oct}$), respectively. Assuming that *absorption* is the dominant sorption process and $MW_{oct}/MW_{OM} = \gamma_{oct}/\gamma_{OM} = 1$, Eq. (8) can then be simplified to

$$Log K_p = Log K_{OA} + Log f_{om} - 11.91 \qquad \text{Equation 9}$$

In opposition to *ab*sorption partitioning (Eq.9), numerous investigations focused on a remarkable role of EC (Elemental Carbon) *ad*sorption in the ambient air. Dachs and Eisenreich (2000) reported evidence for *ad*sorption to EC dominating the partitioning in the New Jersey atmosphere. Based on the assumption that EC is a representative for the particulate phase, the comprehensive gas-particle partition coefficient that explains for both the absorption and adsorption mechanisms are given by (Eq.10):

$$K_P = \frac{f_{OM}MW_{OCT}\zeta_{OCT}}{\rho_{OCT}MW_{OM}\zeta_{OM}10^{12}}K_{OA} + f_{EC}\frac{a_{EC}}{10^{12}a_{AC}}K_{SA} \qquad \text{Equation 10}$$

where f_{EC} is the fraction of elemental carbon in the aerosol (dimensionless), a_{AC} is the surface area of the activated carbon (m^2) and a_{EC} is the specific surface area of the elemental carbon (m^2) (Dachs and Eisenreich, 2000). When the gas-particle partitioning is overwhelmed by both OM

and EC partitioning mechanisms, K_p can be precisely estimated by applying the Dach-Eisenreich model (Eq. 21). Apart from several concerns associated with the reliability of applying diagnostic binary ratios of PAHs, previous studies have shown some promising results for characterizing tsunami backwash deposits (Pongpiachan, 2014; Tipmanee et al., 2012). In this manuscript, eight diagnostic binary ratios namely, Fl/(Fl+Pyr), B[*e*]P/(B[*e*]P+B[*a*]P), B[*b,j,k*]F/B[*g,h,i*]P, Ind/B[*g,h,i*]P, B[*a*]P/B[*e*]P, B[*a*]A/Chry, B[*a*]P/B[*g,h,i*]P and Ind/(Ind+B[*g,h,i*]P), were employed as geochemical tracers to classify their potential origins of sediments collected at the 2004 tsunami affected coastal areas, where sampling positions were clearly described in Table 2 (Tsapakis and Stephanou, 2005; Yunker and Macdonald, 2003). Diagnostic binary ratios of PAHs obtained from this study were also compared with other marine sediments as clearly described in Table 3.

As illustrated in Table 4, the diagnostic binary ratios of Ind/(Ind+B[*g,h,i*]P), B[a]A/Chry, B[a]P/B[g,h,i]P, Fluo/(Fluo+Pyr), B[k]F/Ind and An/(Phe+An) of Khao Lak Coastal Sediments (KLCS), the 2004 tsunami affected area, were computed and compared with other PAH profiles obtained from numerous source types. It appears reasonable to interpret that the average value of Ind/(Ind+B[*g,h,i*]P) (0.34) detected in KLCS can be attributed to mixed sources with binary ratios ranged from 0.2 to 0.5 (Wang et al., 1999). Furthermore, B[a]A/(B[a]A+Chry) (0.49), Fluo/(Fluo+Pyr) (0.35) and An/(Phe+An) (0.11) underlined the impact of crude oil consumptions over KLCS (see Table 4). Although some diagnostic binary ratios show crucial results for characterizing probable origins of PAH congeners, this technique alone coupled with the application of fingerprint should theoretically be applied with the highest attention as numerous processes such as heterogeneous and homogeneous chemical reactions, photodegradation, and microbiological activities can play a significant role in the variations of PAH contents in sediment samples. Therefore, it is also important to find some alternative methods to attenuate the previously discussed ambiguities. In this particular case, the two-dimensional (2D) plots of diagnostic binary ratios can to some extent increase the reliability of binary ratio approach and hence seems rationale to apply for characterization of tsunami backwash deposits.

Additional efforts were performed with the application of 2D plots of An/(An+Phe) and Fluo/(Fluo + Pyr), which exhibits for X-axis and Y-axis, respectively. Diagnostic binary ratios of PAHs in tsunami affected coastal area were compared with those in PM$_{10}$ collected from various emission sources adjacent to the study sites (see Table 5 and Table 6). The most obvious patterns as illustrated in Figure 3 are: (*i*) 2D plots of Non-Pakarang group (i.e. none-tsunami affected area) and other marine deposits were positioned close to each other; (*ii*) there are different PAH sources in Pakarang group (i.e. tsunami affected area) sediments, probably highlighting the impact of Tsunami backwash; (*iii*) 2D plots of Non-Pakarang group were positioned in comparable locations as those of PM$_{10}$ collected from rubber manufacturing factory (RMF), fish can manufacturing factory (CPF), corpse incinerator (CI), para rubber tree burning (PTB) and bush burning (BB) (see Table 7) indicating that PAH congeners were transferred from potential sources in Songkhla province to Khao Lak coastal area then finally to sediments; and (*iv*) 2D plots of Pakarang group is greatly varied from other plot components, which can be interpreted as the deposition of PAH fingerprints buried in terrestrial components triggered by Tsunami backwash in Pakarang area (see Figure 2).

5.3. *Application of principal component analysis (PCA)*

Five components were identified from the principal component matrix each representing 41.80 %, 24.90 %, 15.17 %, 8.69 % and 3.80 % of the variance, thus accounting for 94.36 % of the total variance (Table 8). PC1 shows high loading on high molecular weight PAHs (i.e. B[b]F, B[k]F, B[e]P, B[a]P and Ind). These compounds are typical biomarkers of biomass burning. Thus, it is reasonable to assume that the forest fire govern the spatial distribution of PAHs in this coastal region and explained for 41.80 % source contribution. The relatively high loadings

of D[a,h]A and B[g,h,i]P can be attributed to wood combustion in PC2. On the other hand, PC3 has high loading of Phe and An, followed by the relatively high abundances of Fluo, B[a]A, Chry found in PC4 indicating the signature of "diesel emissions" and "oil combustions" plausibly delivered to the sampling sites via long range transportation and/or the "wash back" of terrestrial components triggered by tsunami. Three dimensional plots of PC1, PC2, and PC3 successfully discriminated the potential tsunami deposit group from the typical marine sediment group as displayed in Figures 4, 5, 6, and 7. In this study, the typical marine sediment group (i.e. 5D, 7, 8D, 9D, 10D, 11D, 14D, 17D, 26D, 39D, 45D, 49D, 53D, 56, 2D, 65D, 74D, 75D) were observed as a "horizontal laid down position", whereas the potential tsunami deposit group (i.e. 31A, 32, 32D, 34D, 35D, 36D, 41D, 42C, 44D, 69D, 70D, 71D, 72-2D, 72bD, 73D) were found as a "horizontal laid up position". Other sediment samples laid down between these two layers were considered as mixture the typical marine sediments and tsunami deposits.

6. Research constraints/limitations and future works

There are many research constraints/limitations and future works that need to be discussed. Firstly, there is some missing elements in the existing research literature associated with the impacts of humic and fulvic acids extracted from tsunami backwash deposits on the apparent water solubility enhancement of PAH congeners. In spite of numerous studies highlight the effects of humic and fulvic acids as natural surfactants that increased the solubility of PAH compounds (Cho et al., 2002; Danielsen et al., 1995; Tanaka et al., 1997), the majority of reports contain results of only modern sediments. According to our best knowledge, there is no studies connected with humic substances and the solubility of PAH congeners in historic tsunami sediments. Secondly, several concerns associated with the application of diagnostic binary ratios for characterizing emission sources of PAH congeners have been previously discussed and thus the application of this approach for characterizing tsunami backwash deposits need to be conducted with great caution (Galarneau, 2008). It is well known that PAH source characteristics are not specific by emission source type. Furthermore, diagnostic binary ratios of PAHs demonstrate substantial intra-source variability and inter-source similarity. For instance, a review (Yunker et al., 2002) highlights binary ratios for Fluo/(Fluo+Pyr), of ≥0.5 for burnings of various types of grass, wood and coal, and finalizes that emission sources are difficult to discriminate even when numerous binary ratios are investigated together. It is also crucial to underline that relative PAH contents are not well preserved in the atmosphere. Several processes such as homogeneous/heterogeneous chemical reaction, gas-particle partitioning, meteorological conditions and wet/dry depositions can dramatically alter PAH contents in the atmosphere (Birgül et al., 2011; Dachs and Eisenreich, 2000; Golomb et al., 2001; Kamens et al., 1988, 1990, 1994; Zhang et al., 2010, 2013). Thirdly, numerous microbiological activities can significantly decrease PAH contents in marine sediments and thus one should interpret diagnostic binary ratios of PAHs with great cautions (Guo et al., 2010; Heitkamp and Cerniglia, 1989; Moody et al., 2004). In this manuscript, the author had reviewed some advantages and disadvantages of using aromatic compounds as an alternative geochemical proxy for characterizing tsunami backwash deposits. The application of PAHs as aromatic tracers assist in an exceeding insights connected with tsunami inundation, sediment transport, and deposition process of tsunami deposits, which can be subject to erosion by tsunami waves and surface runoff by heavy rain in the tsunami-affected coastal areas of Andaman Sea, Thailand.

Declarations

Author contribution statement

Siwatt Pongpiachan: Performed the experiments; Analyzed and interpreted the data; Wrote the paper.

Vanisa Surapipith, Suparerk Aukkaravittayapun, Saran Posh-yachinda: Analyzed and interpreted the data.

Muhammad Zaffar Hashmi: Conceived and designed the experiments; Wrote the paper.

Data availability statement

Data will be made available on request.

Declaration of interests statement

The authors declare no conflict of interest.

Additional information

No additional information is available for this paper.

References

Anyanwu, I.N., Sikoki, F.D., Semple, K.T., 2020. Quantitative assessment data of PAHs and N-PAHs in core sediments from the Niger Delta, Nigeria. Data in Brief 33, 106484.

Atkinson, R., Arey, J., 1994. Atmospheric chemistry of gas-phase polycyclic aromatic hydrocarbons: formation of atmospheric mutagens. Environ. Health Perspect. 102 (Suppl 4), 117.

Atkinson, R., Aschmann, S.M., 1987. Kinetics of the gas-phase reactions of alkylnaphthalenes with O_3, N_2O_5 and OH radicals at 298 ± 2 K. Atmos. Environ. 21 (11), 2,323–2,326.

Baumard, P., Budzinski, H., Garrigues, P., Sorbe, J.C., Burgeot, T., Bellocq, J., 1998a. Concentrations of PAHs (polycyclic aromatic hydrocarbons) in various marine organisms in relation to those in sediment and to trophic level. Mar. Pollut. Bull. 36, 951–960.

Baumard, P., Budzinski, H., Garrigues, P., 1998b. Polycyclic aromatic hydrocarbons in sediments and mussels of the western Mediterranean Sea. Environ. Toxicol. Chem.: Int. J. 17 (5), 765–776.

Bellanova, P., Schwarzbauer, J., Reicherter, K.R., Jaffe, B.E., Szczucinski, W., 2016. Our fingerprint in tsunami deposits-anthropogenic markers as a new tsunami identification tool. In: AGU Fall Meeting Abstracts.

Bellanova, P., Frenken, M., Richmond, B., Schwarzbauer, J., La Selle, S., Griswold, F., Reicherter, K., 2020a. Organic geochemical investigation of far-field tsunami deposits of the Kahana Valley, O'ahu, Hawai'i. Sedimentology 67 (3), 1230–1248.

Bellanova, P., Frenken, M., Reicherter, K., Jaffe, B., Szczuciński, W., Schwarzbauer, J., 2020b. Anthropogenic pollutants and biomarkers for the identification of 2011 Tohoku-oki tsunami deposits (Japan). Mar. Geol. 422, 106117.

Birgül, A., Tasdemir, Y., Cindoruk, S.S., 2011. Atmospheric wet and dry deposition of polycyclic aromatic hydrocarbons (PAHs) determined using a modified sampler. Atmos. Res. 101 (1-2), 341–353.

Budzinski, H., Jones, I., Bellocq, J., Piérard, C., Garrigues, P., 1997. Evaluation of sediment contamination by polycyclic aromatic hydrocarbons in the Gironde estuary. Mar. Chem. 58 (1-2), 85–97.

Cai, X.B., Xue, D., Li, D., Wang, F., Zhao, Z.Y., 2013. Distribution and sources of polycyclic aromatic hydrocarbons in the sediments of Ramsar swamp in inner deep bay of Hong Kong. Environ. Chem. 32, 451–458 (in Chinese).

Calvert, J.G., Atkinson, R., Becker, K.H., Kamens, R.M., Seinfeld, J.H., Wallington, T.H., Yarwood, G.R.E.G., 2002. The Mechanisms of Atmospheric Oxidation of the Aromatic Hydrocarbons. Oxford University Press.

Cantalamessa, G., Di Celma, C., 2005. Sedimentary features of tsunami backwash deposits in a shallow marine Miocene setting, Mejillones Peninsula, northern Chile. Sediment. Geol. 178 (3-4), 259–273.

Cardellicchio, N., Buccolieri, A., Giandomenico, S., Lopez, L., Pizzulli, F., Spada, L., 2007. Organic pollutants (PAHs, PCBs) in sediments from the mar piccolo in taranto (ionian sea, southern Italy). Mar. Pollut. Bull. 55 (10-12), 451–458.

Cerniglia, C.E., 1993. Biodegradation of polycyclic aromatic hydrocarbons. Curr. Opin. Biotechnol. 4 (3), 331–338.

Cerniglia, C.E., Heitkamp, M.A., 1989. Microbial degradation of polycyclic aromatic hydrocarbons (PAH) in the aquatic environment. Metabolism of polycyclic aromatic hydrocarbons in the aquatic environment, pp. 41–68.

Chagué-Goff, C., Niedzielski, P., Wong, H.K., Szczuciński, W., Sugawara, D., Goff, J., 2012. Environmental impact assessment of the 2011 tohoku-oki tsunami on the Sendai plain. Sediment. Geol. 282, 175–187.

Chagué-Goff, C., Wong, H.K., Sugawara, D., Goff, J., Nishimura, Y., Beer, J., Goto, K., 2014. Impact of Tsunami Inundation on Soil Salinisation: up to One Year after the 2011 Tohoku-Oki Tsunami. In: Tsunami Events and Lessons Learned. Springer, Dordrecht, pp. 193–214.

Chagué-Goff, C., Goff, J., Wong, H.K., Cisternas, M., 2015. Insights from geochemistry and diatoms to characterise a tsunami's deposit and maximum inundation limit. Mar. Geol. 359, 22–34.

Chagué-Goff, C., Szczuciński, W., Shinozaki, T., 2017. Applications of geochemistry in tsunami research: a review. Earth Sci. Rev. 165, 203–244.

Chiou, C.T., Malcolm, R.L., Brinton, T.I., Kile, D.E., 1986. Water solubility enhancement of some organic pollutants and pesticides by dissolved humic and fulvic acids. Environ. Sci. Technol. 20 (5), 502–508.

Cho, H.H., Choi, J., Goltz, M.N., Park, J.W., 2002. Combined effect of natural organic matter and surfactants on the apparent solubility of polycyclic aromatic hydrocarbons. J. Environ. Qual. 31 (1), 275–280.

ChooChuay, C., Pongpiachan, S., Tipmanee, D., Deelaman, W., Suttinun, O., Wang, Q., Cao, J., 2020a. Long-range transboundary atmospheric transport of polycyclic aromatic hydrocarbons, carbonaceous compositions, and water-soluble ionic species in southern Thailand. Aerosol Air Quality Res. 20 (7), 1591–1606.

ChooChuay, C., Pongpiachan, S., Tipmanee, D., Suttinun, O., Deelaman, W., Wang, Q., Cao, J., 2020b. Impacts of PM2.5 sources on variations in particulate chemical compounds in ambient air of Bangkok, Thailand. Atmospheric Pollut. Res. 11 (9), 1657–1667.

ChooChuay, C., Pongpiachan, S., Tipmanee, D., Deelaman, W., Iadtem, N., Suttinun, O., Cao, J., 2020c. Effects of agricultural waste burning on PM2. 5-bound polycyclic aromatic hydrocarbons, carbonaceous compositions, and water-soluble ionic species in the ambient air of Chiang-Mai, Thailand. Polycycl. Aromat. Comp. 1–22.

Christensen, B.T., 1992. Physical fractionation of soil and organic matter in primary particle size and density separates. In: Advances in Soil Science. Springer, New York, NY, pp. 1–90.

Cimberle, R.M., Bottino, P., Valerio, F., 1983. Decomposition of benzo[a]pyrene deposited on glass fibre filters and exposed to sunlight. Chemosphere 12 (3), 317–324.

Cornelissen, G., Gustafsson, Ö., Bucheli, T.D., Jonker, M.T., Koelmans, A.A., van Noort, P.C., 2005. Extensive sorption of organic compounds to black carbon, coal, and kerogen in sediments and soils: mechanisms and consequences for distribution, bioaccumulation, and biodegradation. Environ. Sci. Technol. 39 (18), 6881–6895.

Dachs, J., Eisenreich, S.J., 2000. Adsorption onto aerosol soot carbon dominates gas-particle partitioning of polycyclic aromatic hydrocarbons. Environ. Sci. Technol. 34, 3690–3697.

Dahanayake, K., Kulasena, N., Ravi Prasad, G.V., Dutta, K., Ray, D.K., 2012. Sedimentological and 14C dating studies of past tsunami events in Southern Sri Lanka. Nat. Hazards 63, 197–209.

Danielsen, K.M., Chin, Y.P., Buterbaugh, J.S., Gustafson, T.L., Traina, S.J., 1995. Solubility enhancement and fluorescence quenching of pyrene by humic substances: the effect of dissolved oxygen on quenching processes. Environ. Sci. Technol. 29 (8), 2162–2165.

Dawson, A.G., Shi, S., 2000. Tsunami deposits. Pure Appl. Geophys. 157 (6-8), 875–897.

Dawson, A.G., Stewart, I., 2007. Tsunami deposits in the geological record. Sediment. Geol. 200 (3-4), 166–183.

de Maagd, P.G.J., ten Hulscher, D.T.E., van den Heuvel, H., Opperhuizen, A., Sijm, D.T., 1998. Physicochemical properties of polycyclic aromatic hydrocarbons: aqueous solubilities, n-octanol/water partition coefficients, and Henry's law constants. Environ. Toxicol. Chem. 17 (2), 251–257.

Deelaman, W., Pongpiachan, S., Tipmanee, D., Choochuay, C., Iadtem, N., Suttinun, O., Cao, J., 2020. Source identification of polycyclic aromatic hydrocarbons in terrestrial soils in Chile. J. S. Am. Earth Sci. 99, 102514.

Denis, E.H., Toney, J.L., Tarozo, R., Anderson, R.S., Roach, L.D., Huang, Y., 2012. Polycyclic aromatic hydrocarbons (PAHs) in lake sediments record historic fire events: validation using HPLC-fluorescence detection. Org. Geochem. 45, 7–17.

Ellis, D.A., Martin, J.W., Mabury, S.A., Hurley, M.D., Sulbaek Andersen, M.P., Wallington, T.J., 2003. Atmospheric lifetime of fluorotelomer alcohols. Environ. Sci. Technol. 33 (17), 3816–3820.

Fan, Z., Kamens, R.M., Hu, J., Zhang, J., McDow, S., 1996. Photostability of nitro-polycyclic aromatic hydrocarbons on combustion soot particles in sunlight. Environ. Sci. Technol. 30 (4), 1358–1364.

Feldens, P., Schwarzer, K., Szczucinski, W., Stattegger, K., Sakuna, D., Somgpongchaiykul, P., 2009. Impact of 2004 tsunami on seafloor morphology and offshore sediments, Pakarang Cape. Thailand. Pol. J. Environ. Stud. 18 (1).

Finizio, A., Mackay, D., Bidleman, T., Harner, T., 1997. Octanol-air partition coefficient as a predictor of partitioning of semi-volatile organic chemicals to aerosols. Atmos. Environ. 31 (15), 2289–2296.

Gauthier, T.D., Seitz, W.R., Grant, C.L., 1987. Effects of structural and compositional variations of dissolved humic materials on pyrene K_{oc} values. Environ. Sci. Technol. 21 (3), 243–248.

Galarneau, E., 2008. Source specificity and atmospheric processing of airborne PAHs: implications for source apportionment. Atmos. Environ. 42 (35), 8139–8149.

Gogou, A., Stratigakis, N., Kanakidou, M., Stephanou, E.G., 1996. Organic aerosols in Eastern Mediterranean: components source reconciliation by using molecular markers and atmospheric back trajectories. Org. Geochem. 25 (1-2), 79–96.

Gogou, A.I., Apostolaki, M., Stephanou, E.G., 1998. Determination of organic molecular markers in marine aerosols and sediments: one-step flash chromatography compound class fractionation and capillary gas chromatographic analysis. J. Chromatogr. A 799 (1-2), 215–231.

Goldstein, A.H., Wofsy, S.C., Spivakovsky, C.M., 1995. Seasonal variations of nonmethane hydrocarbons in rural New England: constraints on OH concentrations in northern midlatitudes. J. Geophys. Res. 100 (D10), 21023–21033.

Golomb, D., Barry, E., Fisher, G., Varanusupakul, P., Koleda, M., Rooney, T., 2001. Atmospheric deposition of polycyclic aromatic hydrocarbons near New England coastal waters. Atmos. Environ. 35 (36), 6245–6258.

Goto, K., Chagué-Goff, C., Fujino, S., Goff, J., Jaffe, B., Nishimura, Y., Witter, R.C., 2011. New insights of tsunami hazard from the 2011 Tohoku-oki event. Mar. Geol. 290 (1-4), 46–50.

Goto, T., Satake, K., Sugai, T., Ishibe, T., Harada, T., Gusman, A.R., 2019. Tsunami history over the past 2000 years on the Sanriku coast, Japan, determined using gravel deposits to estimate tsunami inundation behavior. Sediment. Geol. 382, 85–102.

Guo, C., Dang, Z., Wong, Y., Tam, N.F., 2010. Biodegradation ability and dioxgenase genes of PAH-degrading Sphingomonas and Mycobacterium strains isolated from mangrove sediments. Int. Biodeterior. Biodegrad. 64 (6), 419–426.

He, X., Pang, Y., Song, X., Chen, B., Feng, Z., Ma, Y., 2014. Distribution, sources and ecological risk assessment of PAHs in surface sediments from Guan River Estuary, China. Mar. Pollut. Bull. 80 (1-2), 52–58.

Heitkamp, M.A., Cerniglia, C.E., 1989. Polycyclic aromatic hydrocarbon degradation by a Mycobacterium sp. in microcosms containing sediment and water from a pristine ecosystem. Appl. Environ. Microbiol. 55 (8), 1968.

Irizuki, T., Fujiwara, O., Yoshioka, K., Suzuki, A., Tanaka, Y., Nagao, M., Nishimura, O., 2019. Geochemical and micropaleontological impacts caused by the 2011 Tohoku-oki tsunami in Matsushima Bay, northeastern Japan. Mar. Geol. 407, 261–274.

Ishiyama, T., Goto, K., Yokoyama, Y., Goff, J., 2020. Dating tsunami deposits: present knowledge and challenges. Earth Sci. Rev. 200, 102971.

Jahromi, F.A., Moore, F., Keshavarzi, B., Mohebbi-Nozar, S.L., Mohammadi, Z., Sorooshian, A., Abbasi, S., 2020. Bisphenol A (BPA) and polycyclic aromatic hydrocarbons (PAHs) in the surface sediment and bivalves from Hormozgan Province coastline in the Northern Persian Gulf: a focus on source apportionment. Mar. Pollut. Bull. 152, 110941.

Jayawardana, D.T., Ishiga, H., Pitawala, H.M.T.G.A., 2012. Geochemistry of surface sediments in tsunami-affected Sri Lankan lagoons regarding environmental implications. Int. J. Environ. Sci. Technol. 9, 41–55.

Jiao, L., Meng, W., Zheng, B., Zhang, L., Zhao, X., Qin, Y., 2010. Distribution of polycyclic aromatic hydrocarbons (PAHs) in different size fractions of sediments from intertidal zone of Bohai Bay, China. China Environ. Sci. 30 (9), 1241–1248.

Judd, K., Chagué-Goff, C., Goff, J., Gadd, P., Zawadzki, A., Fierro, D., 2017. Multi-proxy evidence for small historical tsunamis leaving little or no sedimentary record. Mar. Geol. 385, 204–215.

Junge, C.E., 1977. Basic considerations about trace constituents in the atmosphere as related to the fate of global pollutants. In: Suffet, I.H. (Ed.), Fate of Pollutants in the Air and Water Environments. John Wiley, New York, pp. 25–77.

Kalaitzoglou, M., Terzi, E., Samara, C., 2004. Patterns and sources of particle-phase aliphatic and polycyclic aromatic hydrocarbons in urban and rural sites of western Greece. Atmos. Environ. 38, 2545–2560.

Kamens, R., Perry, J.M., Saucy, D.A., Bell, D.A., Newton, D.L., Brand, B., 1985. Factors which influence polycyclic aromatic hydrocarbon decomposition on wood smoke particles. Environ. Int. 11, 131–136.

Kamens, R., Guo, Z., Fulcher, J.N., Bell, D.A., 1988. The influence of humidity, sunlight, and temperature on the daytime decay of polyaromatic hydrocarbons on atmospheric soot particles. Environ. Sci. Technol. 22, 103–112.

Kamens, R., Guo, J., Guo, M., McDow, S.R., 1990. Polynuclear aromatic hydrocarbon degradation by heterogeneous reactions with N₂O₅ on atmospheric particles. Atmos. Environ. 24A, 1161–1173.

Kamens, R.M., Fan, Z.F., Yao, Y., Chen, D., Chen, S., Vartianinen, M., 1994. A methodology for modeling the formation and decay of nitro-PAH in the atmosphere. Chemosphere 28, 1623–1632.

Kamlet, M.J., Doherty, R.M., Carr, P.W., Mackay, D., Abraham, M.H., Taft, R.W., 1988. Linear solvation energy relationships. 44. Parameter estimation rules that allow accurate prediction of octanol/water partition coefficients and other solubility and toxicity properties of polychlorinated biphenyls and polycyclic aromatic hydrocarbons. Environ. Sci. Technol. 22 (5), 503–509.

Kim, E.J., Oh, J.E., Chang, Y.S., 2003. Effects of forest fire on the level and distribution of PCDD/Fs and PAHs in soil. Sci. Total Environ. 311 (1-3), 177–189.

Kozak, K., Ruman, M., Kosek, K., Karasiński, G., Stachnik, Ł., Polkowska, Ż., 2017. Impact of volcanic eruptions on the occurrence of PAHs compounds in the aquatic ecosystem of the southern part of west spitsbergen (hornsund fjord, svalbard). Water 9 (1), 42.

Kukkonen, J., Landrum, P.F., 1996. Distribution of organic carbon and organic xenobiotics among different particle-size fractions in sediments. Chemosphere 32 (6), 1063–1076.

Lang, Y., Wang, N., Gao, H., Bai, J., 2012. Distribution and risk assessment of polycyclic aromatic hydrocarbons (PAHs) from Liaohe estuarine wetland soils. Environ. Monit. Assess. 184 (9), 5545–5552.

Lee, W., Stevens, S.P., Hites, A.R., 2003. Rate constants for the gas-phase reactions of methylphenanthrenes with OH as a function of temperature. J. Phys. Chem. 107, 6603–6608.

Liu, Y., Chen, L., Huang, Q.H., Li, W.Y., Tang, Y.J., Zhao, J.F., 2009. Source apportionment of polycyclic aromatic hydrocarbons (PAHs) in surface sediments of the Huangpu River, Shanghai, China. Sci. Total Environ. 407 (8), 2931–2938.

Lohmann, R., MacFarlane, J.K., Gschwend, P.M., 2005. Importance of black carbon to sorption of native PAHs, PCBs, and PCDDs in Boston and New York harbor sediments. Environ. Sci. Technol. 39 (1), 141–148.

Lu, G.N., Dang, Z., Tao, X.Q., Yang, C., Yi, X.Y., 2008. Estimation of water solubility of polycyclic aromatic hydrocarbons using quantum chemical descriptors and partial least squares. Mol. Inform. 27 (5), 618–626.

May, W.E., Wasik, S.P., Freeman, D.H., 1978. Determination of the solubility behavior of some polycyclic aromatic hydrocarbons in water. Anal. Chem. 50 (7), 997–1000.

Moreira, S., Costa, P.J., Andrade, C., Lira, C.P., Freitas, M.C., Oliveira, M.A., Reichart, G.J., 2017. High resolution geochemical and grain-size analysis of the AD 1755 tsunami deposit: insights into the inland extent and inundation phases. Mar. Geol. 390, 94–105.

Miller, D.J., Hawthorne, S.B., Gizir, A.M., Clifford, A.A., 1998. Solubility of polycyclic aromatic hydrocarbons in subcritical water from 298 K to 498 K. J. Chem. Eng. Data 43 (6), 1043–1047.

Millet, D.B., Goldstein, H.A., Allan, D.J., Bates, S.T., Boudries, H., Bower, N.K., Coe, H., Ma, Y., McKay, M., Quinn, K.P., Sullivan, A., Weber, J.R., Worsnop, R.D., 2004. Volatile organic compound measurements at Trinidad Head, California during ITCT 2K2: analysis of sources, atmospheric composition and aerosol residence times. J. Geophys. Res. 109, D23S16.

Minoura, K., Nakaya, S., Sato, H., 1987. Traces of tsunamis recorded in lake deposits. An ex-ample from Jusan, Shiura-mura, Aomori. J. Seismol. Soc. Jpn. 40, 183–196 (in Japanese with English abstract).

Minoura, K., Nakata, T., 1994. Discovery of an ancient tsunami deposit in coastal sequences of southwest Japan: verification of a large historic tsunami. Isl. Arc 3, 66–72.

Minoura, K., Nakaya, S., 1991. Traces of tsunami preserved in inter-tidal lacustrine and marsh deposits: some examples from northeast Japan. J. Geol. 99, 265–287.

Moody, J.D., Freeman, J.P., Fu, P.P., Cerniglia, C.E., 2004. Degradation of benzo[a] pyrene by Mycobacterium vanbaalenii PYR-1. Appl. Environ. Microbiol. 70 (1), 340–345.

Olivella, M.A., Ribalta, T.G., De Febrer, A.R., Mollet, J.M., De Las Heras, F.X.C., 2006. Distribution of polycyclic aromatic hydrocarbons in riverine waters after Mediterranean forest fires. Sci. Total Environ. 355 (1-3), 156–166.

Ollivon, D., Blanchoud, H., Motelay-Massei, A., Garban, B., 2002. Atmospheric deposition of PAHs to an urban site, Paris, France. Atmos. Environ. 36 (17), 2891–2900.

Pankow, J.F., 1994. An absorption model of gas/particle partitioning of organic compounds in the atmosphere. Atmos. Environ. 28 (2), 185–188.

Pongpiachan, S., 2009. Application of cloud point extraction for the determination of pyrene in natural water. SE. Asian. J. Trop. Med. 40 (2), 392–400.

Pongpiachan, S., Bualert, S., Sompongchaiyakul, P., Kositanont, C., 2009. Factors affecting sensitivity and stability of polycyclic aromatic hydrocarbons determined by gas chromatography quadrupole ion trap mass spectrometry. Anal. Lett. 42 (13), 2106–2130.

Pongpiachan, S., 2010. Atmospheric lifetimes and traveling distances of airborne carcinogenic polycyclic aromatic hydrocarbons. Chin. J. Clin. 16 (7), 830–837.

Pongpiachan, S., 2013a. Fingerprint of carcinogenic semi-volatile organic compounds (SVOCs) during bonfire night. Asian Pac. J. Cancer Prev. APJCP 14 (5), 3243–3254.

Pongpiachan, S., 2013b. Vertical distribution and potential risk of particulate polycyclic aromatic hydrocarbons in high buildings of Bangkok, Thailand. Asian Pac. J. Cancer Prev. APJCP 14 (3), 1865–1877.

Pongpiachan, S., 2013c. Diurnal variation, vertical distribution and source apportionment of carcinogenic polycyclic aromatic hydrocarbons (PAHs) in Chiang-mai, Thailand. Asian Pac. J. Cancer Prev. APJCP 14 (3), 1851–1863.

Pongpiachan, S., Tipmanee, D., Deelaman, W., Muprasit, J., Feldens, P., Schwarzer, K., 2013a. Risk assessment of the presence of polycyclic aromatic hydrocarbons (PAHs) in coastal areas of Thailand affected by the 2004 tsunami. Mar. Pollut. Bull. 76 (1-2), 370–378.

Pongpiachan, S., Thumanu, K., Phatthalung, W., Tipmanee, D., Kanchai, P., Feldens, P., Schwarzer, K., 2013b. Using Fourier transform infrared (FTIR) to characterize tsunami deposits in near-shore and coastal waters of Thailand. Sci. Tsunami Hazards 32 (1), 39–57.

Pongpiachan, S., Thumanu, K., Tanthanuch, W., Tipmanee, D., Kanchai, P., Schwarzer, K., Tancharakorn, S., 2013c. Sedimentary features of tsunami backwash deposits as assessed by micro-beam synchrotron X-ray fluorescence (μ-SXRF) at the Siam photon laboratory. Sci. Tsunami Hazards 32 (2), 96–115.

Pongpiachan, S., Choochuay, C., Hattayanone, M., Kositanont, C., 2013d. Temporal and spatial distribution of particulate carcinogens and mutagens in Bangkok, Thailand. Asian Pac. J. Cancer Prev. APJCP 14 (3), 1879–1887.

Pongpiachan, S., Ho, K.F., Cao, J., 2013e. Estimation of gas-particle partitioning coefficients (Kp) of carcinogenic polycyclic aromatic hydrocarbons by carbonaceous aerosols collected at Chiang-mai, Bangkok and hat-Yai, Thailand. Asian Pac. J. Cancer Prev. APJCP 14 (4), 3369–3384.

Pongpiachan, S., 2014. Application of binary diagnostic ratios of polycyclic aromatic hydrocarbons for identification of tsunami 2004 backwash sediments in khao lak, Thailand. Sci. World J.

Pongpiachan, S., Hattayanone, M., Tipmanee, D., Suttinun, O., Khumsup, C., Kittikoon, I., Hirunyatrakul, P., 2018. Chemical characterization of polycyclic aromatic hydrocarbons (PAHs) in 2013 Rayong oil spill-affected coastal areas of Thailand. Environ. Pollut. 233, 992–1002.

Pongpiachan, S., Surapipith, V., Hashmi, M.Z., Latif, M., Sohail, M., Eqani, S.A.M.A.S., Promdee, K., 2020. Latitudinal transects and quantitative ecological risk assessments of polycyclic aromatic hydrocarbons in terrestrial soils of Pakistan and king George Island, Antarctica. Polycycl. Aromat. Comp. 1–20.

Prasath, P., Khan, T.H., 2008. Impact of Tsunami on the heavy metal accumulation in water, Sediments and fish at Poompuhar coast, Southeast Coast of India. J. Chem. 5 (1), 16–22.

Sahu, S.K., Pandit, G.G., 2003. Estimation of octanol-water partition coefficients for polycylic aromatic hydrocarbons using reverse-phase HPLC. J. Liq. Chromatogr. Relat. Technol. 26 (1), 135–146.

Sakuna, D., Szczucinski, W., Feldens, P., Schwarzer, K., Khokiattiwong, S., 2012. Sedimentary deposits left by the 2004 Indian Ocean tsunami on the inner continental shelf offshore of Khao Lak, Andaman Sea (Thailand). Earth Planets Space 64, 931–943.

Sanders, G., Jones, K.C., Hamilton-Taylor, J., 1993. A simple method to assess the susceptibility of polynuclear aromatic hydrocarbons to photolytic decomposition. *Atmos. Environ., Part A.* General Topics 27 (2), 139–144.

Sander, S.P., 2000. Chemical Kinetics and Photochemical Data for Use in Atmospheric Studies: Evaluation Number 14. JPL Publication, Jet Propulsion Lab., Pasadena, Calif., pp. 2–25

Sany, S.B.T., Hashim, R., Salleh, A., Safari, O., Mehdinia, A., Rezayi, M., 2014. Risk assessment of polycyclic aromatic hydrocarbons in the West Port semi-enclosed basin (Malaysia). Environ. Earth Sci. 71 (10), 4319–4332.

Shi, S., Dawson, A.G., Smith, D.E., 1995. Coastal sedimentation associated with the December 12th, 1992 tsunami in Flores, Indonesia. In: Tsunamis: 1992–1994, pp. 525–536. Birkhäuser Basel.

Sicre, M.A., Marty, J.C., Saliot, A., Aparicio, X., Grimalt, J., Albaiges, J., 1987. Aliphatic and aromatic hydrocarbons in different sized aerosols over the Mediterranean Sea: occurrence and origin. Atmos. Environ. 21 (10), 2247–2259.

Simcik, M.F., Eisenreich, S.J., Lioy, P.J., 1999. Source apportionment and source/sink relationships of PAHs in the coastal atmosphere of Chicago and Lake Michigan. Atmos. Environ. 33 (30), 5071–5079.

Siripong, A., 2006. Andaman seacoast of Thailand field survey after the December 2004 Indian Ocean tsunami. Earthq. Spectra 22 (S3), 187–202.

Sojinu, O.S., Sonibare, O.O., Zeng, E.Y., 2011. Concentrations of polycyclic aromatic hydrocarbons in soils of a mangrove forest affected by forest fire. Toxicol. Environ. Chem. 93 (3), 450–461.

Somboonna, N., Wilantho, A., Jankaew, K., Assawamakin, A., Sangsrakru, D., Tangphatsornruang, Tongsima, S., 2014. Microbial ecology of Thailand tsunami and non-tsunami affected terrestrials. PloS One 9 (4), e94236.

Spivakovsky, C.M., Yevich, R., Logan, A.J., Wofsy, C.S., McElroy, B.M., Prather, J.M., 1990. Tropospheric OH in a 3-dimensional chemical tracer model: an assessment based on observations of CH_3CCl_3. J. Geophys. Res. 95 (D11), 18,441–18,471.

Stout, S.A., Magar, V.S., Uhler, R.M., Ickes, J., Abbott, J., Brenner, R., 2001. Characterization of naturally-occurring and anthropogenic PAHs in urban sediments-Wycoff/Eagle harbor superfund site. Environ. Forensics 2 (4), 287–300.

Stracquadanio, M., Dinelli, E., Trombini, C., 2003. Role of volcanic dust in the atmospheric transport and deposition of polycyclic aromatic hydrocarbons and mercury. J. Environ. Monit. 5 (6), 984–988.

Sugawara, D., Takahashi, T., Imamura, F., 2014. Sediment transport due to the 2011 Tohoku-oki tsunami at Sendai: results from numerical modeling. Mar. Geol. 358, 18–37.

Szczuciński, W., Niedzielski, P., Rachlewicz, G., Sobczyński, T., Zioła, A., Kowalski, A., Siepak, J., 2005. Contamination of tsunami sediments in a coastal zone inundated by the 26 December 2004 tsunami in Thailand. Environ. Geol. 49 (2), 321–331.

Szczuciński, W., Niedzielski, P., Kozak, L., Frankowski, M., Zioła, A., Lorenc, S., 2007. Effects of rainy season on mobilization of contaminants from tsunami deposits left in a coastal zone of Thailand by the 26 December 2004 tsunami. Environ. Geol. 53 (2), 253–264.

Szczuciński, W., 2012. The post-depositional changes of the onshore 2004 tsunami deposits on the Andaman Sea coast of Thailand. Nat. Hazards 60 (1), 115–133.

Szczucinski, W., Pawlowska, J., Lejzerowicz, F., Nishimura, Y., Kokocinski, M., Majewski, W., Nakamura, Y., Pawlowski, J., 2016. Ancient sedimentary DNA reveals past tsunami deposits. Mar. Geol. 381, 29–33.

Tanaka, S., Oba, K., Fukushima, M., Nakayasu, K., Hasebe, K., 1997. Water solubility enhancement of pyrene in the presence of humic substances. Anal. Chim. Acta 337 (3), 351–357.

Tipmanee, D., Deelaman, W., Pongpiachan, S., Schwarzer, K., Sompongchaiyakul, P., 2012. Using polycyclic aromatic hydrocarbons (PAHs) as a chemical proxy to indicate tsunami 2004 backwash in khao lak coastal area, Thailand. Nat. Hazard. Earth. Sys. 12 (5), 1441–1451.

Tsapakis, M., Stephanou, G.E., 2005. Occurrence of gaseous and particulate polycyclic aromatic hydrocarbons in the urban atmosphere: study of sources and ambient temperature effect on the gas/particle concentration and distribution. Environ. Pollut. 133 (1), 147–156.

Tsuji, Y., Namegaya, Y., Matsumoto, H., Iwasaki, S.I., Kanbua, W., Sriwichai, M., Meesuk, V., 2006. The 2004 Indian tsunami in Thailand: surveyed runup heights and tide gauge records. Earth Planets Space 58 (2), 223–232.

Vergnoux, A., Malleret, L., Asia, L., Doumenq, P., Theraulaz, F., 2011. Impact of forest fires on PAH level and distribution in soils. Environ. Res. 111 (2), 193–198.

Vigliotti, L., Andrade, C., Conceição, F., Capotondi, L., Gallerani, A., Bellucci, L.G., 2019. Paleomagnetic, rock magnetic and geochemical study of the 1755 tsunami deposit at Boca do Rio (Algarve, Portugal). Palaeogeogr. Palaeocl. 514, 550–566.

Vila-Escalé, M., Vegas-Vilarrúbia, T., Prat, N., 2007. Release of polycyclic aromatic compounds into a Mediterranean creek (Catalonia, NE Spain) after a forest fire. Water Res. 41 (10), 2171–2179.

Wang, Z., Fingas, M., Shu, Y.Y., Sigouin, L., Landriault, M., Lambert, P., Mullin, J., 1999. Quantitative characterization of PAHs in burn residue and soot samples and differentiation of pyrogenic PAHs from petrogenic PAHs– the 1994 mobile burn study. Environ. Sci. Technol. 33 (18), 3100–3109.

Wang, C.X., Zhang, X.Y., Chen, F.R., 2001. Distribution and partitioning of polycyclic aromatic hydrocarbons (PAHs) in different size fractions in sediments from Boston Harbor, United States. Mar. Pollut. Bull. 42 (11), 1139–1149.

Wang, Z., Liu, Z., Yang, Y., Li, T., Liu, M., 2012. Distribution of PAHs in tissues of wetland plants and the surrounding sediments in the Chongming wetland, Shanghai, China. Chemosphere 89 (3), 221–227.

Wang, P., Mi, W., Xie, Z., Tang, J., Apel, C., Joerss, H., Zhang, Q., 2020. Overall comparison and source identification of PAHs in the sediments of European baltic and North seas, Chinese bohai and Yellow seas. Sci. Total Environ. 737, 139535.

Watanabe, M., Goto, K., Bricker, J.D., Imamura, F., 2018. Are inundation limit and maximum extent of sand useful for differentiating tsunamis and storms? An example from sediment transport simulations on the Sendai Plain, Japan. Sediment. Geol. 364, 204–216.

Watanabe, T., Tsuchiya, N., Yamasaki, S.I., Sawai, Y., Hosoda, N., Nara, F.W., Komai, T., 2020. A geochemical approach for identifying marine incursions: implications for tsunami geology on the Pacific coast of northeast Japan. Appl. Geochem. 104644.

Westerholm, R., Almen, J., Li, H., Rannug, U., Rosen, A., 1992. Exhaust emissions from gasoline-fuelled light duty vehicles operated in different driving conditions: a chemical and biological characterization. Atmos. Environ. 26B, 79–90.

Xue, R., Chen, L., Lu, Z., Wang, J., Yang, H., Zhang, J., Cai, M., 2016. Spatial distribution and source apportionment of PAHs in marine surface sediments of Prydz Bay, East Antarctica. Environ. Pollut. 219, 528–536.

Yamei, H., Zheng, M., Zhengtao, L., Lirong, G., 2009. Distribution of polycyclic aromatic hydrocarbons in sediments from Yellow river estuary and Yangtze river estuary, China. J. Environ. Sci. 21 (12), 1625–1631.

Yang, W., Lang, Y., Li, G., 2014. Cancer risk of polycyclic aromatic hydrocarbons (PAHs) in the soils from Jiaozhou Bay wetland. Chemosphere 112, 289–295.

Yoshii, T., Tanaka, S., Matsuyama, M., 2018. Tsunami inundation, sediment transport, and deposition process of tsunami deposits on coastal lowland inferred from the Tsunami Sand Transport Laboratory Experiment (TSTLE). Mar. Geol. 400, 107–118.

Yunker, B.M., Macdonald, W.R., Vingarzan, R., Mitchell, H.R., Goyette, D., Sylvestre, S., 2002. PAHs in the Fraser River basin: a critical appraisal of PAH ratios as indicators of PAH source and composition. Org. Geochem. 33, 489–515.

Yunker, B.M., Macdonald, W.R., 2003. Petroleum biomarker sources in suspended particulate matter and sediments from the Fraser River Basin and Strait of Georgia, Canada. Org. Geochem. 34, 1525–1541.

Yunker, M.B., Belicka, L.L., Harvey, H.R., Macdonald, R.W., 2005. Tracing the inputs and fate of marine and terrigenous organic matter in Arctic Ocean sediments: a multivariate analysis of lipid biomarkers. Deep-Sea Res. 52 (24-26), 3478–3508.

Yunker, M.B., Macdonald, R.W., Snowdon, L.R., Fowler, B.R., 2011. Alkane and PAH biomarkers as tracers of terrigenous organic carbon in Arctic Ocean sediments. Org. Geochem. 42 (9), 1109–1146.

Zeng, X.K., Li, F.L., Zhou, K., Yang, J.D., Hao, W.L., Zan, Q.J., 2013. Distribution of polycyclic aromatic hydrocarbons (PAHs) in the sediments and mangrove plants at Baguang wetland. Shenzhen. Environ. Sci. Technol 36, 368–373.

Zhang, Y., Yang, B., Meng, J., Gao, S., Dong, X., Shu, J., 2010. Homogeneous and heterogeneous reactions of phenanthrene with ozone. Atmos. Environ. 44 (5), 697–702.

Zhang, Y., Shu, J., Zhang, Y., Yang, B., 2013. Homogeneous and heterogeneous reactions of anthracene with selected atmospheric oxidants. J. Environ. Sci. 25 (9), 1817–1823.

Zhuang, W.E., Wang, X.X., Yao, M.S., Yang, L., Song, X.K., Gong, Z.B., 2011. Distribution and source of polycyclic aromatic hydrocarbons in the surface sediments of Quanzhou Bay China., Environmental Chemistry. Environ. Chem. 30, 928–934 (in Chinese).